# Wind information from Aeolus

EUMETSAT/ECMWF NWP-SAF Satellite Data Assimilation training course, 2024

by Michael Rennie* (m.rennie@ecmwf.int)

Thanks for material from colleagues at ECMWF, ESA and **Aeolus DISC** (particularly DLR)

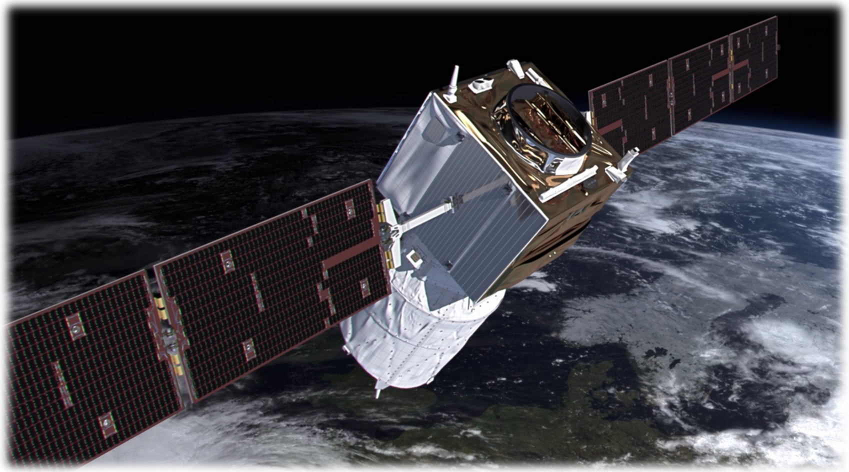

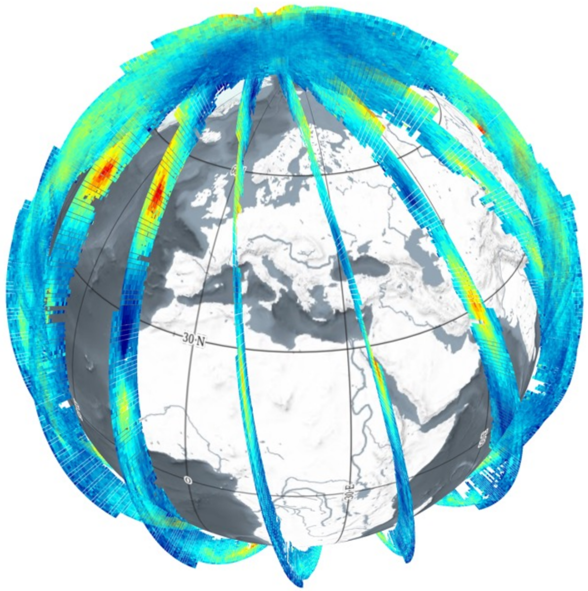


*Actively sensed Observations Team, Earth System Assimilation Section

ECMWF

esa European Space Agency

aeolus

DISC

# An introduction to Aeolus

## Aeolus satellite mission

- **E**uropean **S**pace **A**gency "*Earth Explorer*" mission to measure profiles of wind globally
  - Chosen in 1999
  - Named from Greek mythology: "Keeper of the Winds"

- Payload: Doppler wind lidar (DWL); ALADIN: **A**tmospheric **LA**ser **D**oppler **IN**strument
- **Technology demonstration**; 3-years
- Satellite and instrument built by Airbus Defence and Space
- Status of mission:
  - Launched on **22 August 2018** (10 yr delay due to technical issues!)
  - **First wind lidar in space** and first European lidar in space
  - Measured winds from 3 September 2018 until 5 July 2023. Exceeded nominal mission lifetime; deorbited on 28 July 2023 (lack of fuel!)

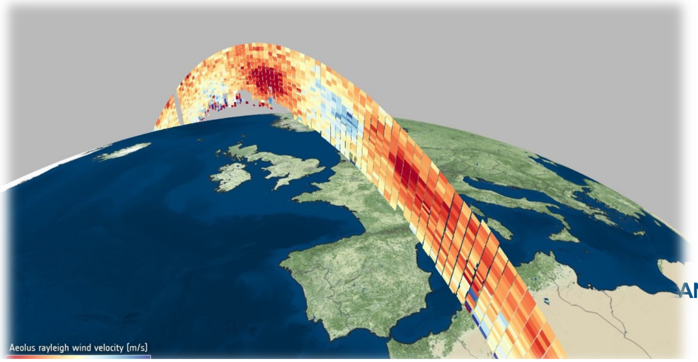


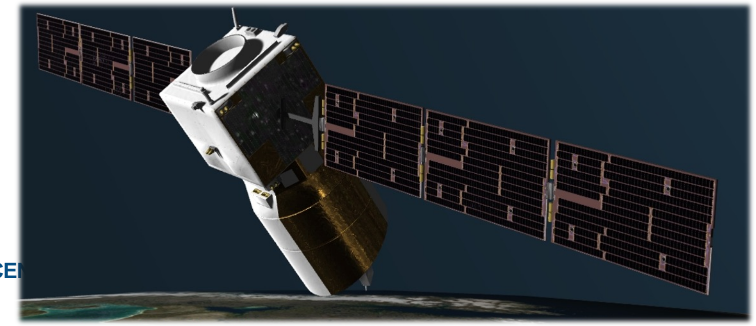

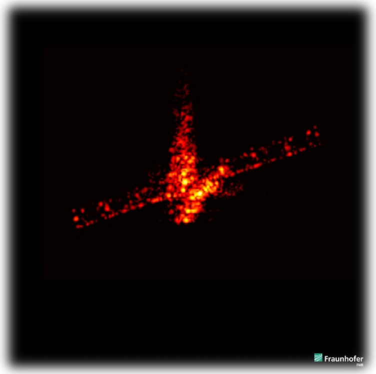

# ESA-developed Earth Observation missions

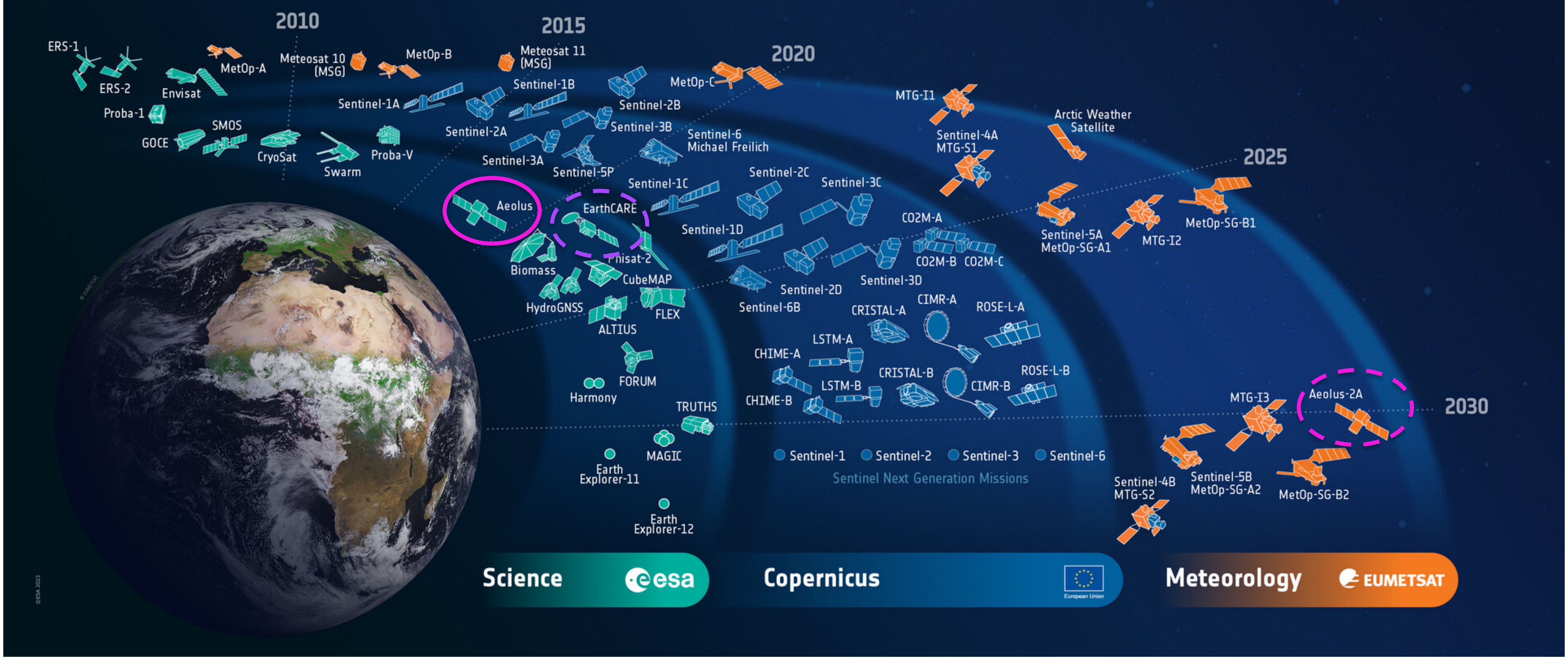

# Aeolus satellite mission

**Scientific Objectives:**

1. **Improve the quality of weather forecasts** by providing **global profile measurements of horizontal line-of-sight wind** in troposphere and lower stratosphere
2. To advance understanding of atmospheric dynamics and climate processes

**Long-term goal:**

**Demonstrate** space-based Doppler wind lidar's capability for operational use

- Global Observing System **still** lacks globally distributed **wind profiles**
- Best NWP impact was expected in **tropics** due to **lack of conventional wind profiles** and atmospheric **dynamical arguments** on importance of wind versus mass (T, p) information near equator

**Geostrophic adjustment theory**

Rossby radius of deformation: $R = \frac{\sqrt{gh}}{2\Omega sin\Phi}$

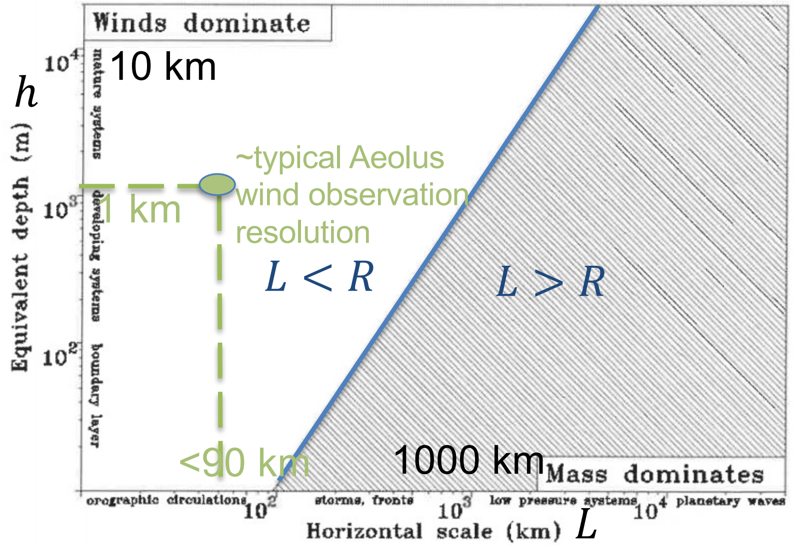


*Figure 2.3. Rossby radius of deformation for a latitude of 45° as a function of horizontal scale and equivalent depth. Open area denotes the range within which the wind field dominates the atmospheric dynamics, and three-dimensional wind measurements are important.*

courtesy: ESA, 1999

## Aeolus measurement principle

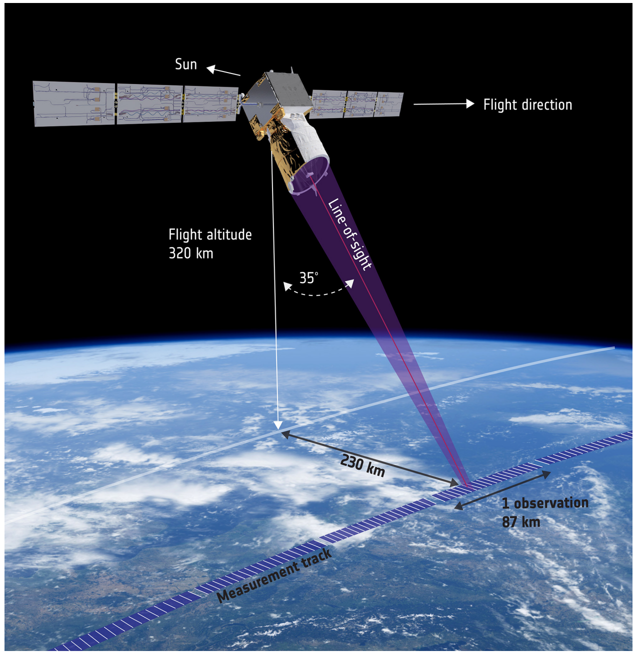


## Coverage in a day

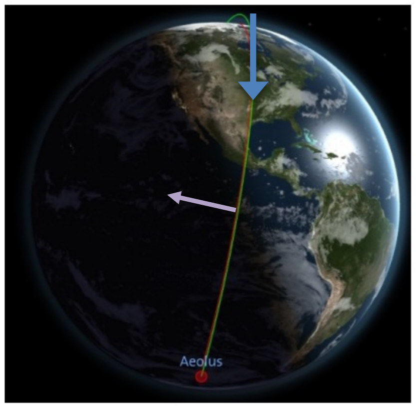


- **Satellite: sun-synchronous, dawn-dusk** (06/18 Local Solar Time) near **polar orbit**; 111 orbits per week
  - *At terminator between day/night to keep solar panels illuminated and minimise reflected solar radiation (noise)*
- **Instrument:**
  - *Direct detection* **Doppler wind lidar** at ~355 nm (long wave ultraviolet), fires ~50 **laser** pulses per second
  - Two receiver channels:
    - **Mie** to determine winds from **cloud** and **aerosol** backscatter ("cloudy"-air)
    - **Rayleigh** to determine winds from **molecular** backscatter (clear-air)
  - Lidar line-of-sight points:
    - 35° off-nadir to determine **horizontal line-of-sight wind component** *(not vector wind)*
    - Perpendicular to satellite-earth relative velocity
    - To **dark side** to minimise reflected solar radiation

# Introduction to lidar, Doppler wind lidar and Aeolus' specific design

# Active optical remote sensing

## Lidar (light detection and ranging)

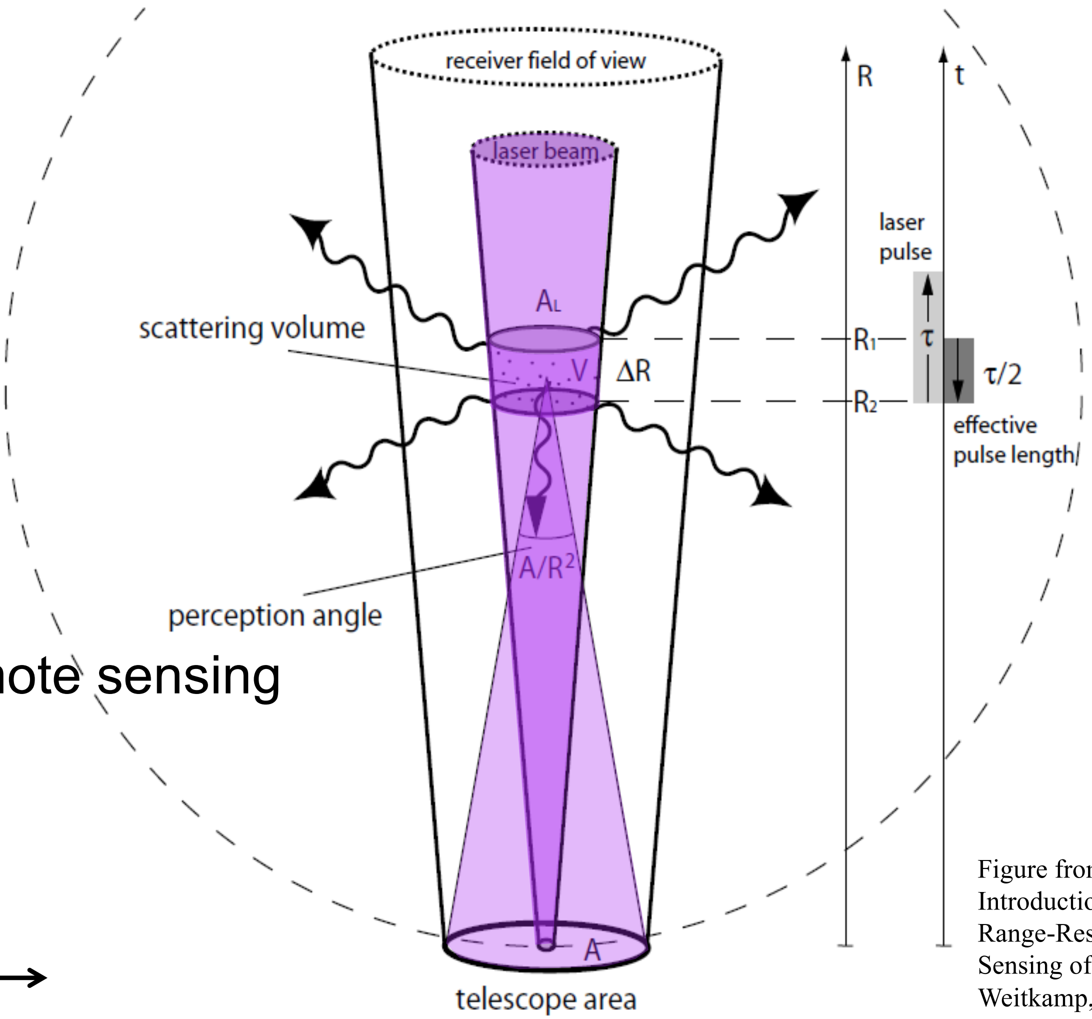


Monostatic design

Bistatic design

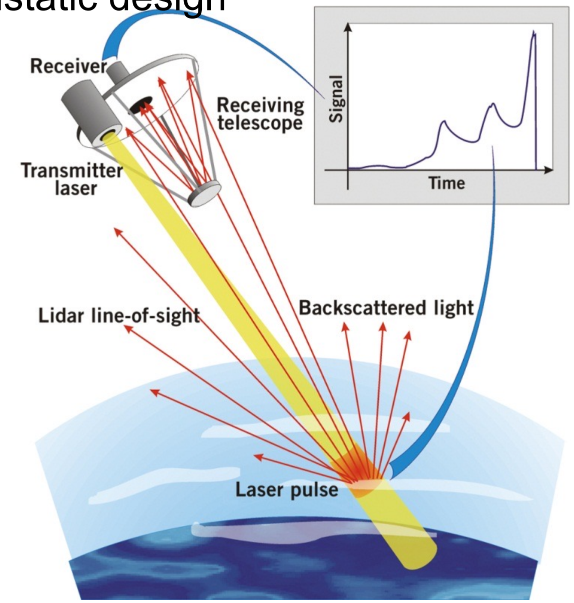


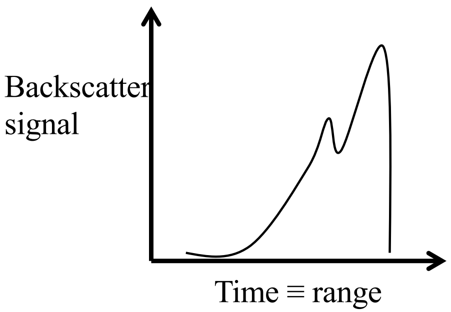


Figure from Wandinger, U. (2005), Introduction to lidar, in LIDAR—Range-Resolved Optical Remote Sensing of the Atmosphere, edited by C. Weitkamp, pp. 1–18, Springer, New York.

## Lidar equation

- Total scattered **power received by lidar** at a time corresponding to range *R* is:

$$P(\lambda, R) = P_L \frac{A_0}{R^2} \xi(\lambda, R) \beta(\lambda, R) T^2(\lambda, R) \frac{c\tau_L}{2}$$

- $\lambda$ = laser wavelength
- $R$ = range of scatterer from sensor
- $\beta$ = **atmosphere** volume backscattering coefficient
- $T$ = one way transmission factor (Beer-Lambert law): $T(\lambda, R) = e^{-\int_0^R \alpha(\lambda,R)dR}$
- $\alpha$ = **atmosphere** attenuation coefficient
- $P_L$ = average power in laser pulse
- $A_0$= area of objective lens
- $c$ = speed of light
- $\tau_L$ = laser pulse duration
- $\xi$ = calibration factor (depending on spectral transmission of receiver and overlap factor)

***Source:*** *Measures (1992); R.M. Measures, "Laser Remote Sensing. Fundamentals and Applications". John Wiley & Sons, 1984*

# “Lidar curtain” of space-borne lidar (CALIPSO (532 nm)), attenuated backscatter: $\beta T^2$

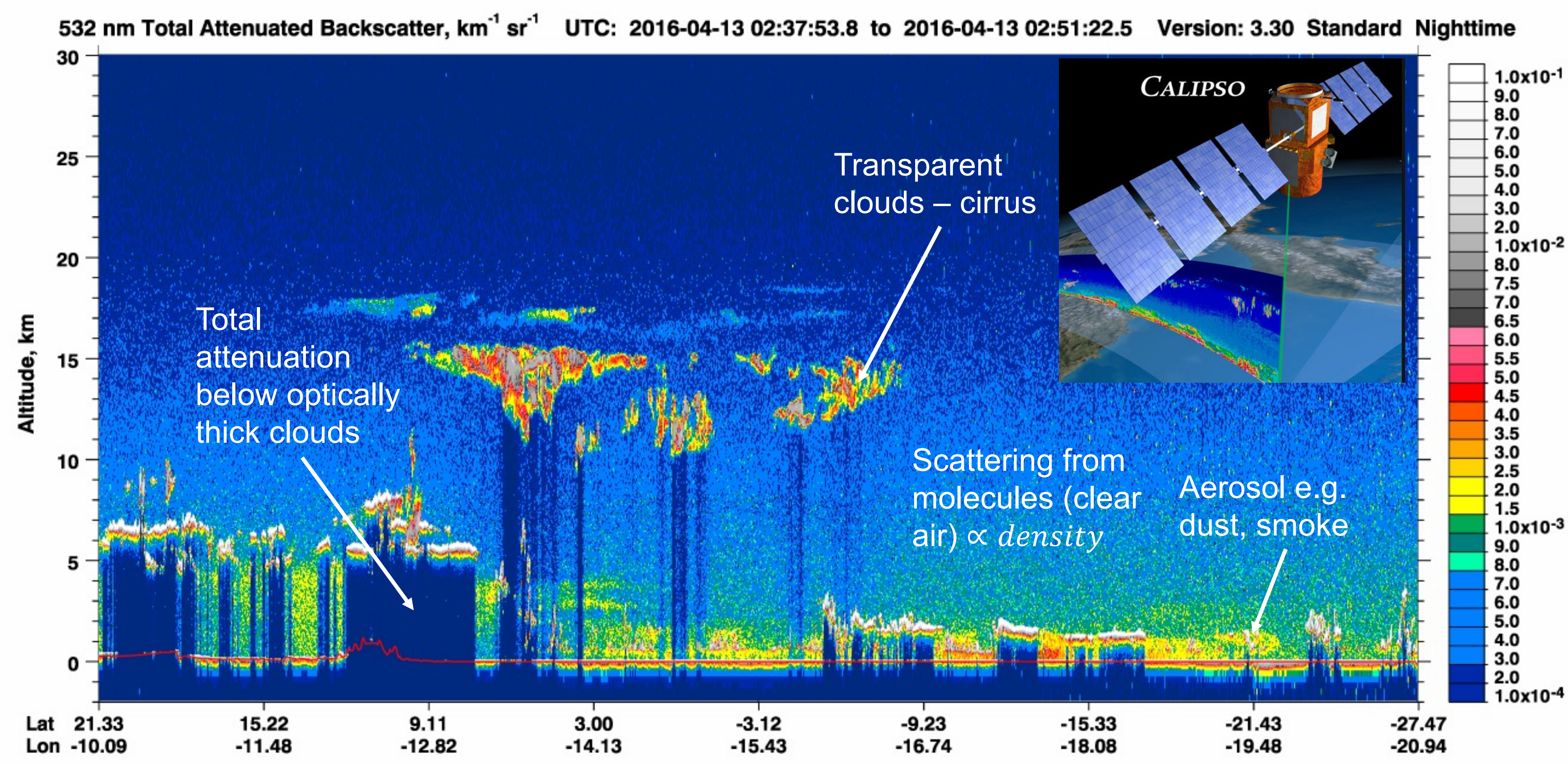


A very successful NASA mission lasting from 2006 to 2023!!

# What’s different about a *Doppler* lidar?

- Atmospheric composition lidars use **amplitude of backscatter signal** and **polarisation** to provide information about the **atmospheric composition**
- **Doppler lidars** measure **change in the frequency** (Doppler shift) of received relative to emitted light **to determine line-of-sight wind**
  - Aeolus also provides an **atmospheric composition** product; a useful demonstration of space-based high-spectral resolution (HSRL) UV lidar; ESA’s EarthCARE **ATLID** lidar will specialise in this

*Aeolus L2A optical properties*
*https://doi.org/10.1029/2020GL092194*

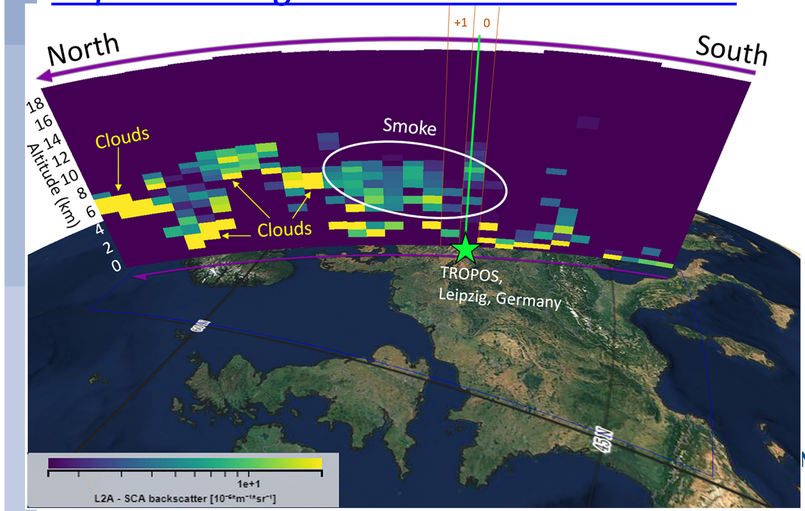


Aeolus Rayleigh backscatter, Hunga-Tonga eruption

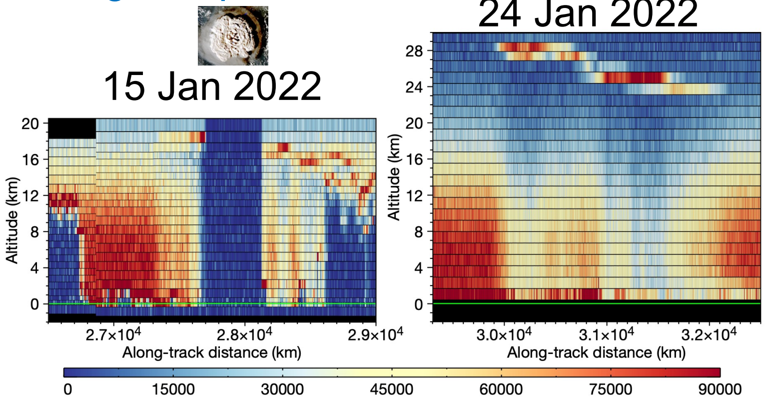


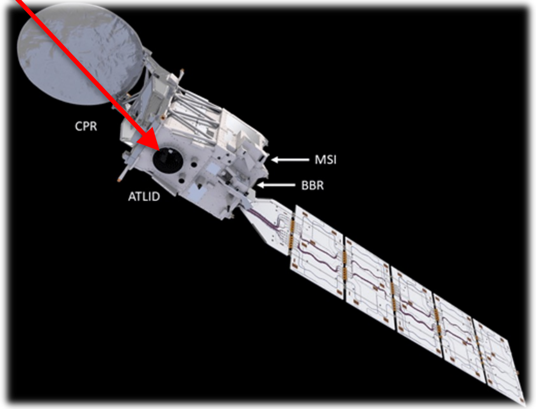

# Doppler wind lidar

A DWL measures the Doppler frequency shift of backscattered light

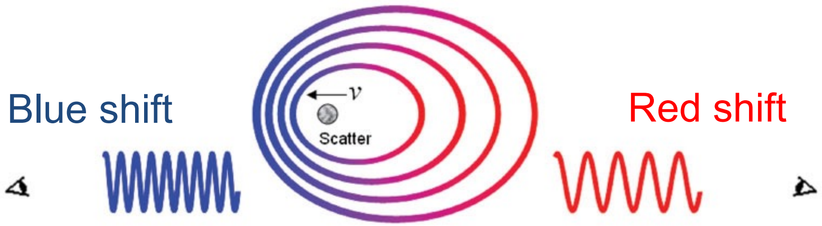


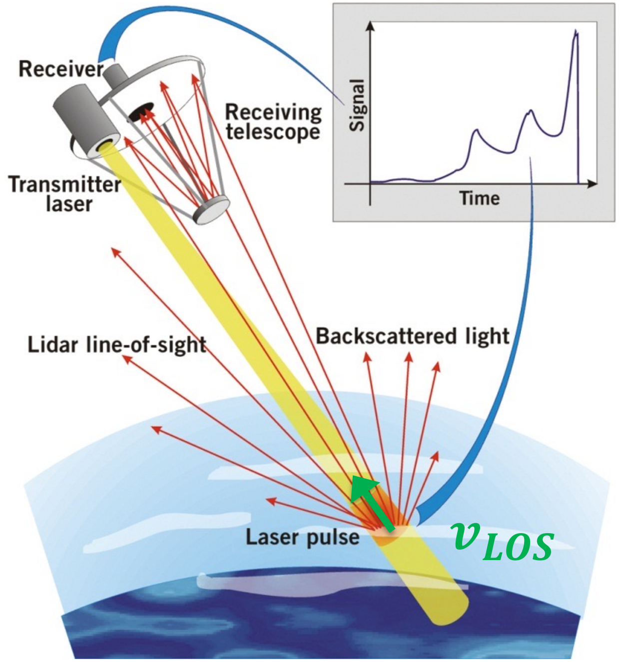


- Doppler frequency shift: $\Delta \boldsymbol{f} = 2\boldsymbol{f_0}\boldsymbol{v_{LOS}}/\boldsymbol{c}$
  - $\Delta \boldsymbol{f}$ = change in frequency
  - $\boldsymbol{f_0}$ = emitted frequency e.g. ~$845$ THz for Aeolus
  - $\boldsymbol{c}$ = speed of light
  - $\boldsymbol{v_{LOS}}$ = component of atmosphere's wind velocity along line-of-sight direction. Average speed of molecules/particles in volume of air.
- Doppler shift frequency is very small, $\frac{\Delta f}{f_0} \approx 10^{-8}$ for 1 m/s LOS wind change; need **very sensitive instrument**
- Backscatter comes from:
  - Air molecules (clear air), particles (aerosol/cloud) and **Earth's surface**

# Aeolus operates lidar at 355 nm wavelength – scattering behaviour

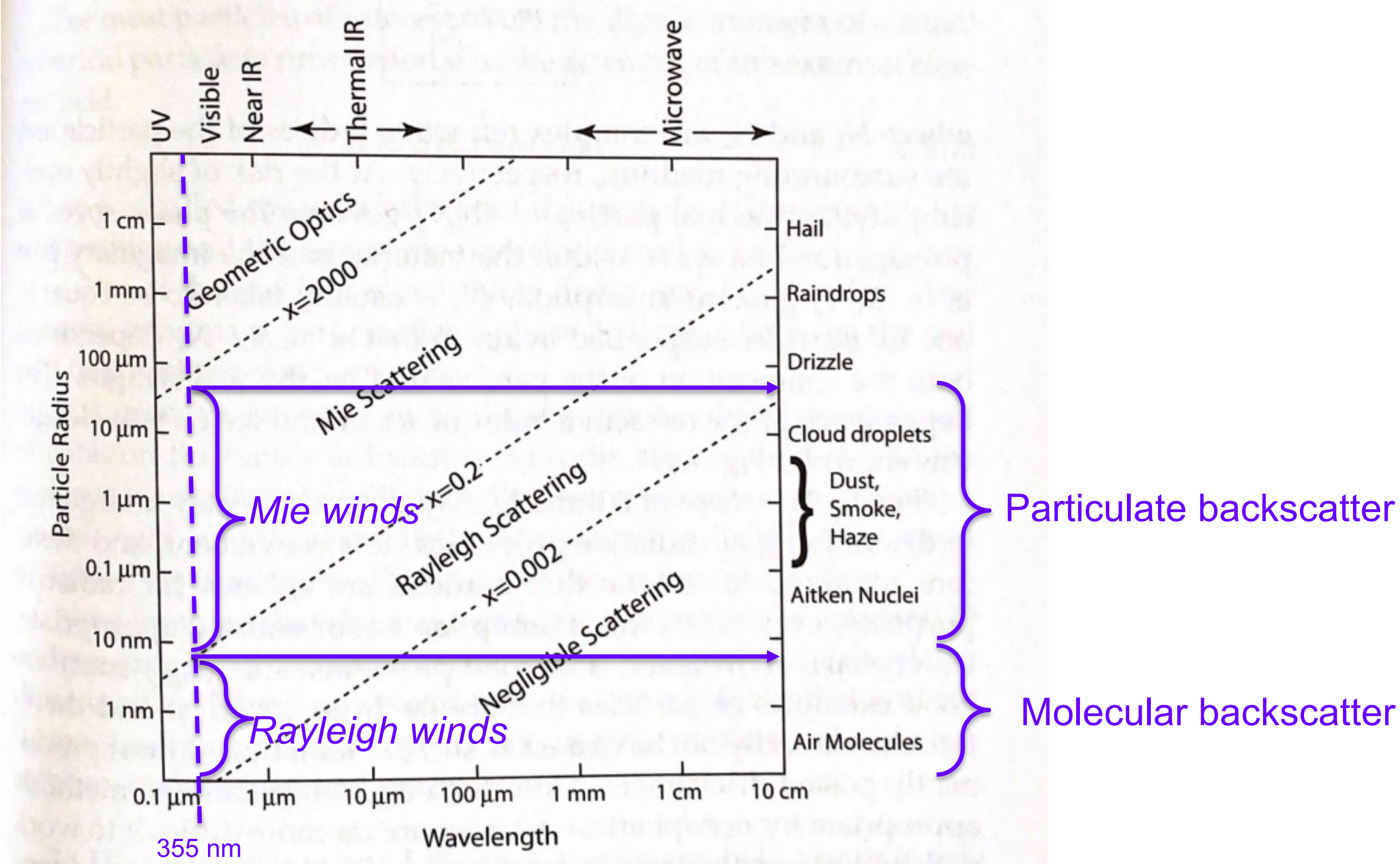


**Fig. 12.1:** Relationship between particle size, radiation wavelength and scattering behavior for atmospheric particles. Diagonal dashed lines represent rough boundaries between scattering regimes.

*Figure from: A First Course in Atmospheric Radiation, G. Petty*

# Winds from **clear sky** conditions; **Rayleigh** scattering

- For Rayleigh scattering: $I \propto \frac{1}{\lambda^4}$; scatterer size $< \frac{\lambda}{10}$
  - For strong scattering from air molecules need short wavelength, *hence Aeolus uses* ***UV laser***
- **Thermal motion** of molecules leads to **Doppler broadening**
  - e.g. T=15 °C get $\sigma_v$=459 m/s!
  - Brillouin scattering effect due to acoustic waves (at higher pressure) also matters
- Wind measured as frequency shift in mean of broadened spectrum (1 m/s HLOS wind=3 MHz $\Delta f$)

credit: Wikipedia

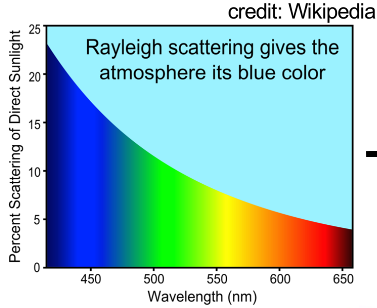


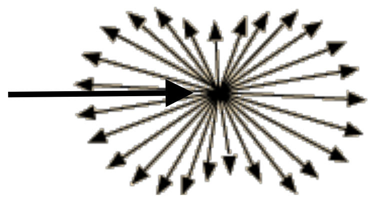

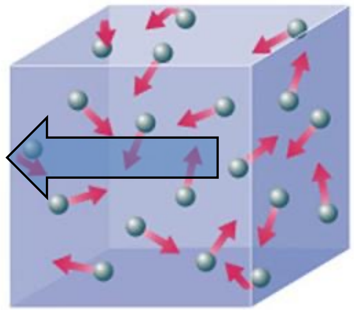

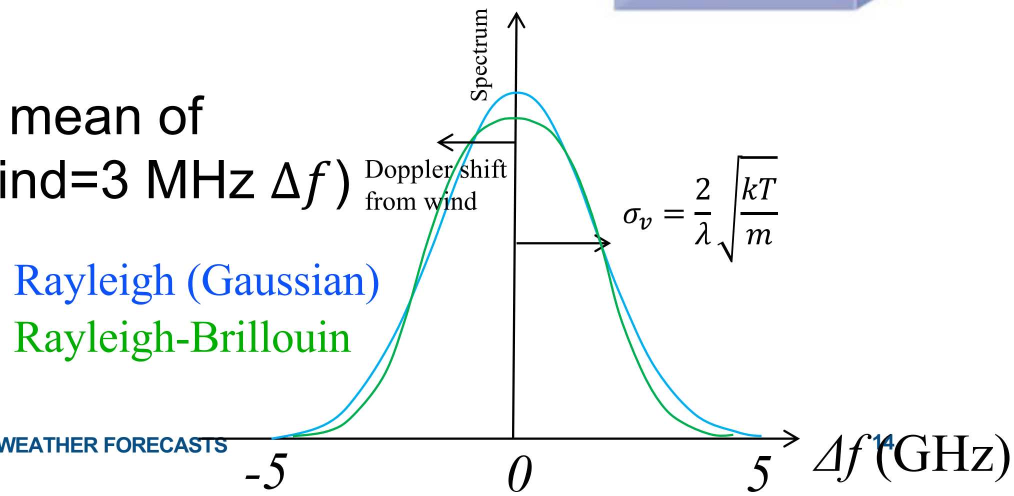

## Winds from “**cloudy**” conditions i.e. scattering from cloud water/ice droplets and aerosols; **Mie** scattering

- Particle sizes ≥ $\lambda$; intensity weakly dependent on $\lambda$
- Doppler broadening negligible (particles “heavy”)
  - Narrow spectrum
  - *No temperature, pressure dependence*
- Wind measured as frequency shift in mean of narrow Mie spectrum
- Since light is strongly attenuated by most clouds, then measure winds mostly from the top of clouds (from space)

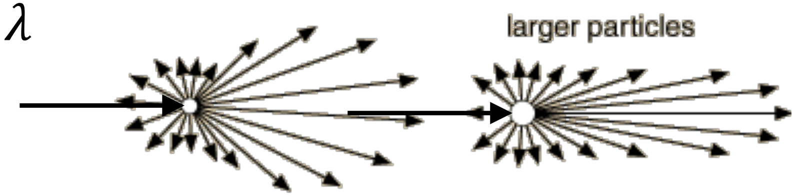


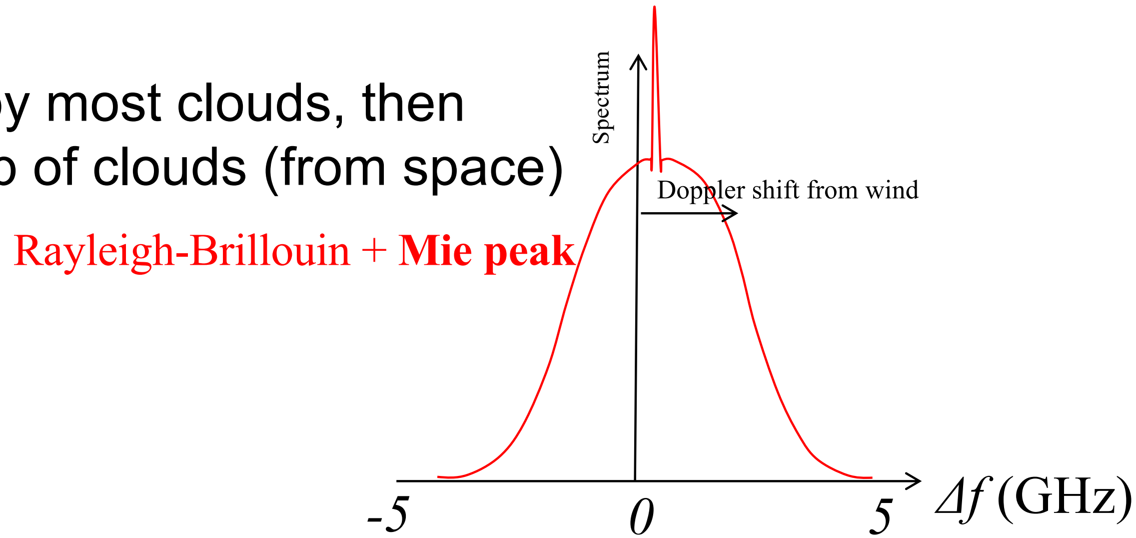

# Aeolus's payload: ALADIN: Atmospheric LAser Doppler Instrument

credit: ESA/Airbus

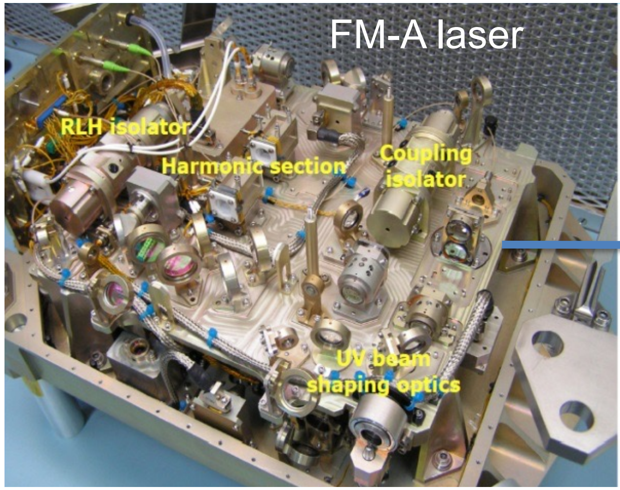


***Complicated optical instrument!***

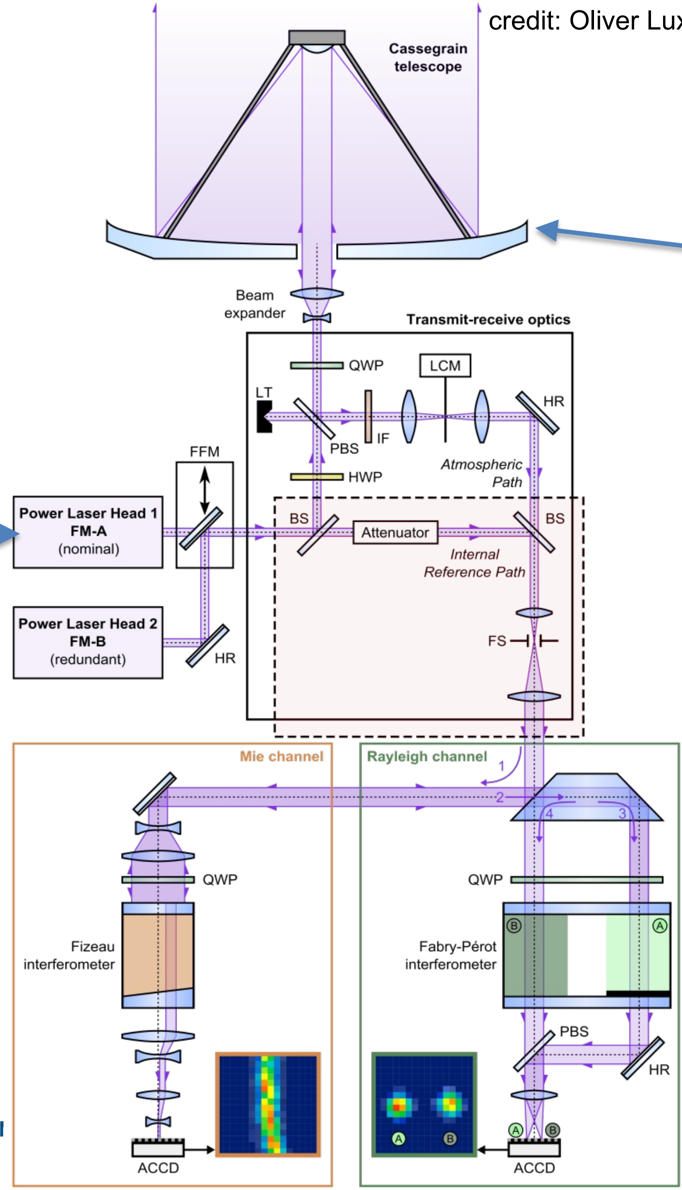


credit: Oliver Lux (DLR)


credit: ESA/Airbus

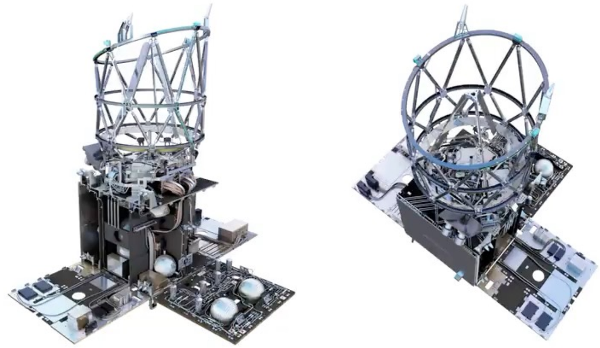

# Rayleigh channel method

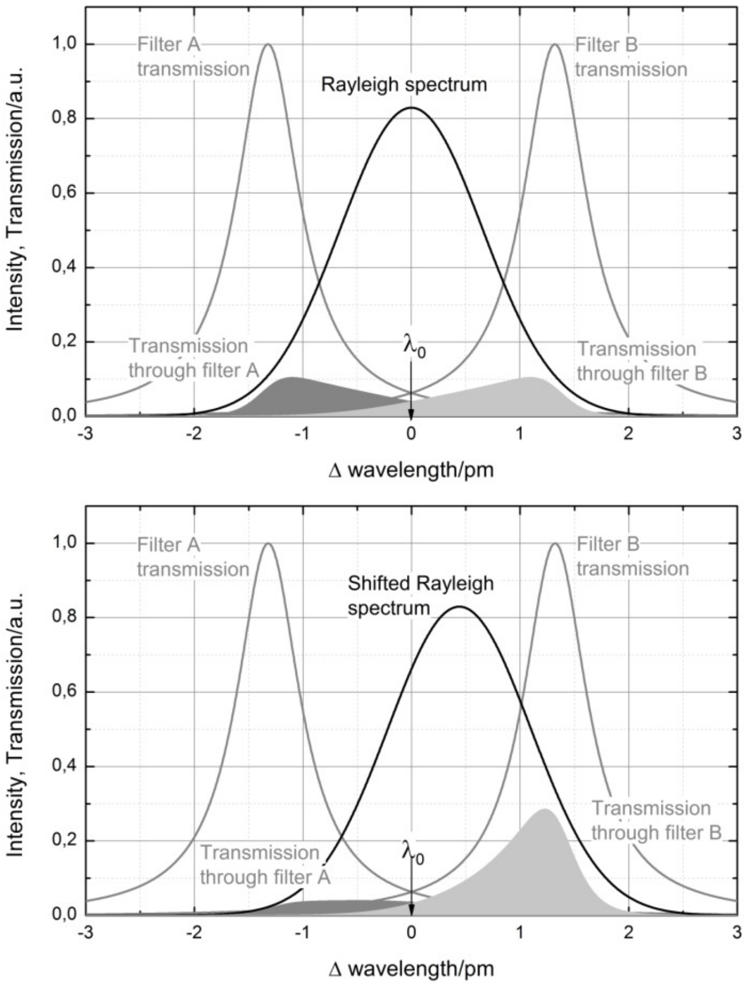


From Reitebuch (2012): Wind Lidar for Atmospheric Research, in Springer Series

**Doube-edge Fabry-Pérot interferometer**

- transmission maximum occurs for a specific wavelength of light; which differs for each interferometer

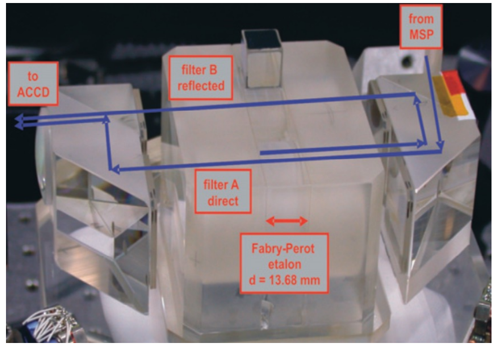


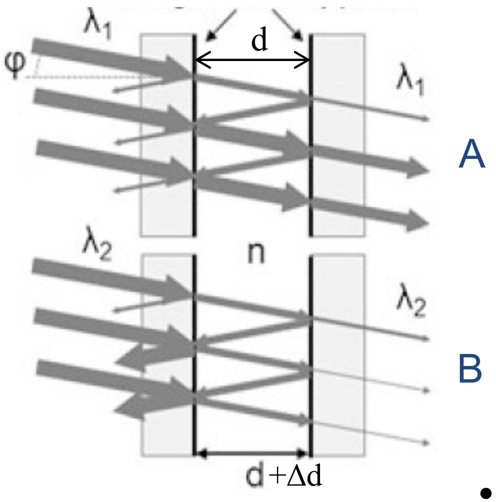


Figure from Reitebuch (2012) The Spaceborne Wind Lidar Mission ADM-Aeolus, Springer

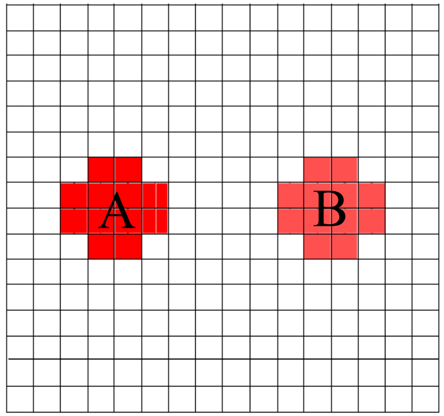


- Rayleigh spots imaged on accumulation CCD
- Contrast of spots $R = \frac{A-B}{A+B}$ calibrated against frequency

# *Real* Rayleigh channel signals (L1B data) over an orbit

Channel A signal photon (*electron*) counts

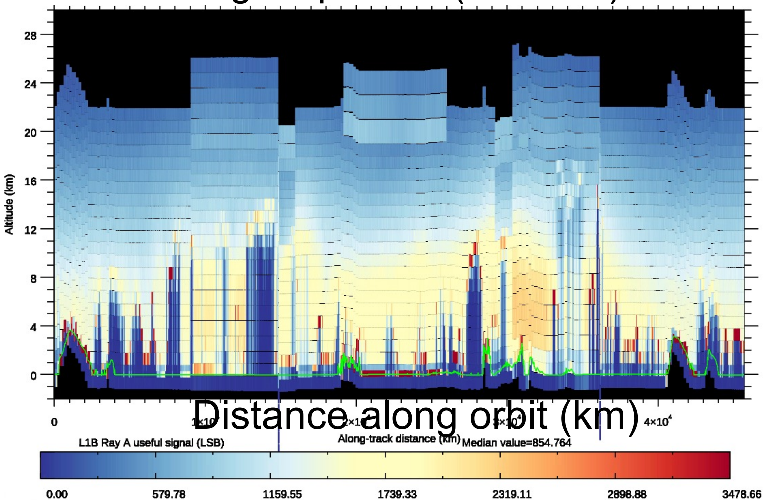


Channel B signal photon counts

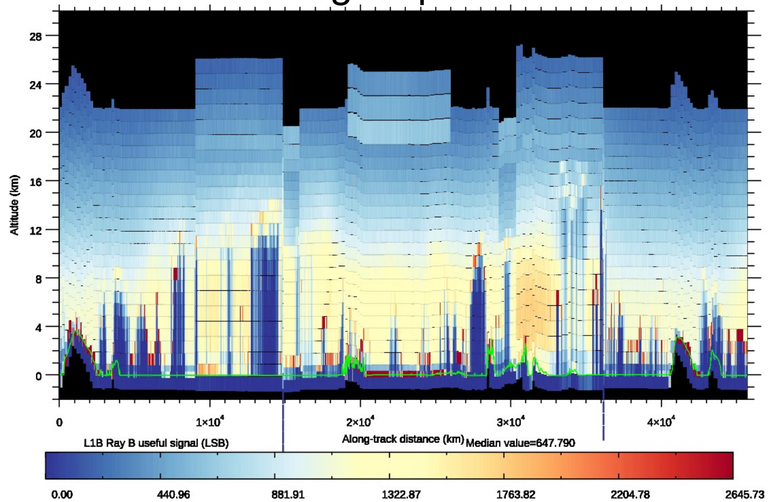


Rayleigh response ∝ Doppler shift

$$R = \frac{A-B}{A+B}$$

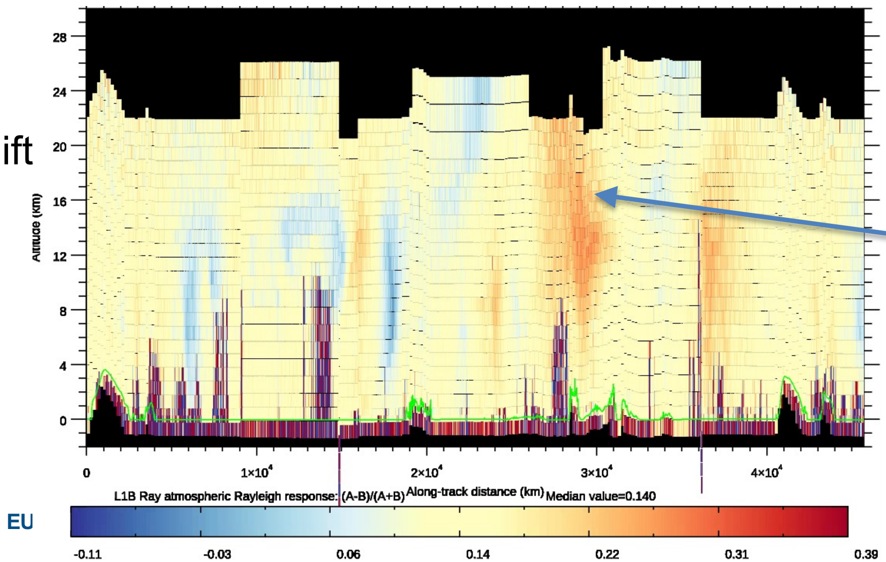


Can see variations in Rayleigh response due to horizontal wind

# Mie channel method

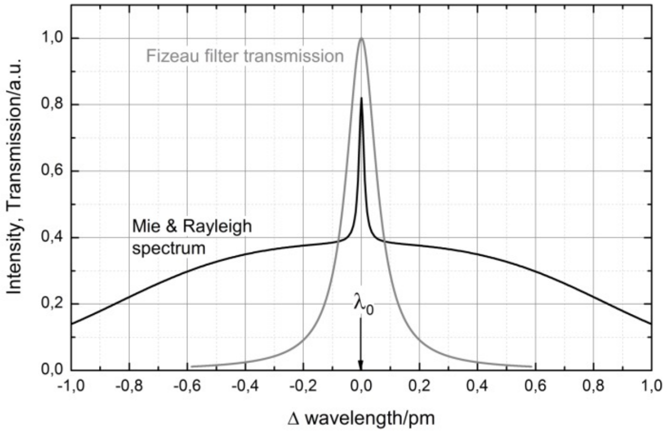


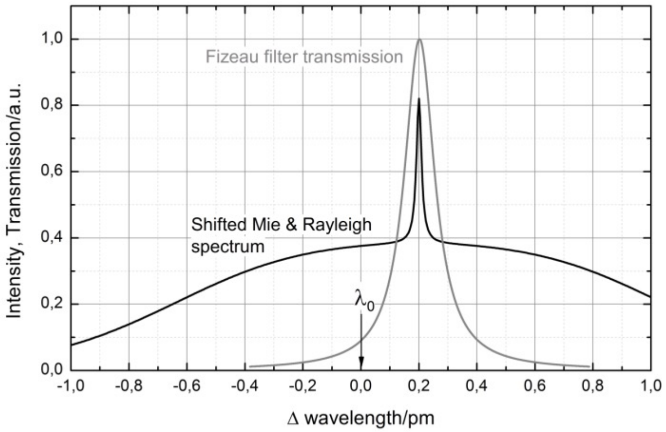


Figure from Reitebuch (2012): Wind Lidar for Atmospheric Research, in Springer Series

## Mie fringe on ACCD

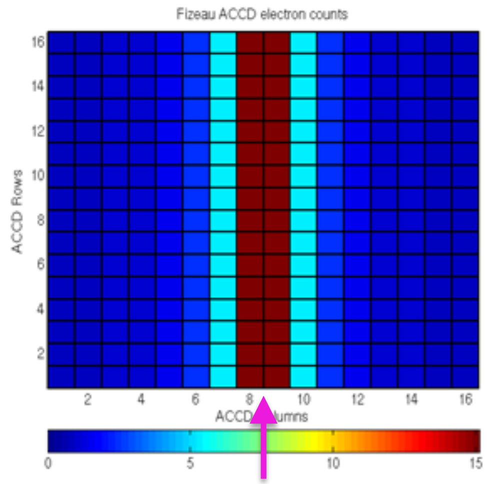


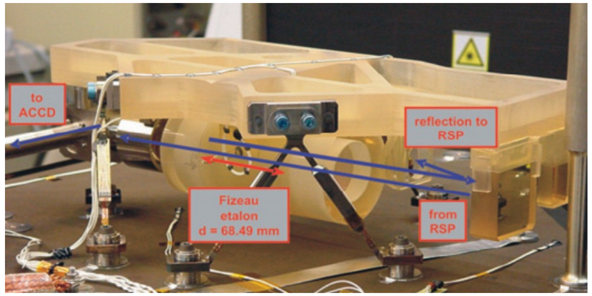


Fringe position $\propto f$, calibration required

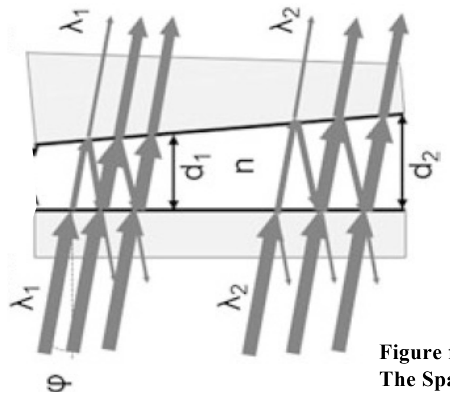


- Narrowband **Fizeau interferometer**
- Transmission max. for *f* depends on x-position – thickness of gap (*wedge* shape)

Figure from Reitebuch (2012) The Spaceborne Wind Lidar Mission ADM-Aeolus, Springer

# *Real* Mie channel signals (L1B data) over an orbit

Mie fringe peak position ∝ Doppler shift

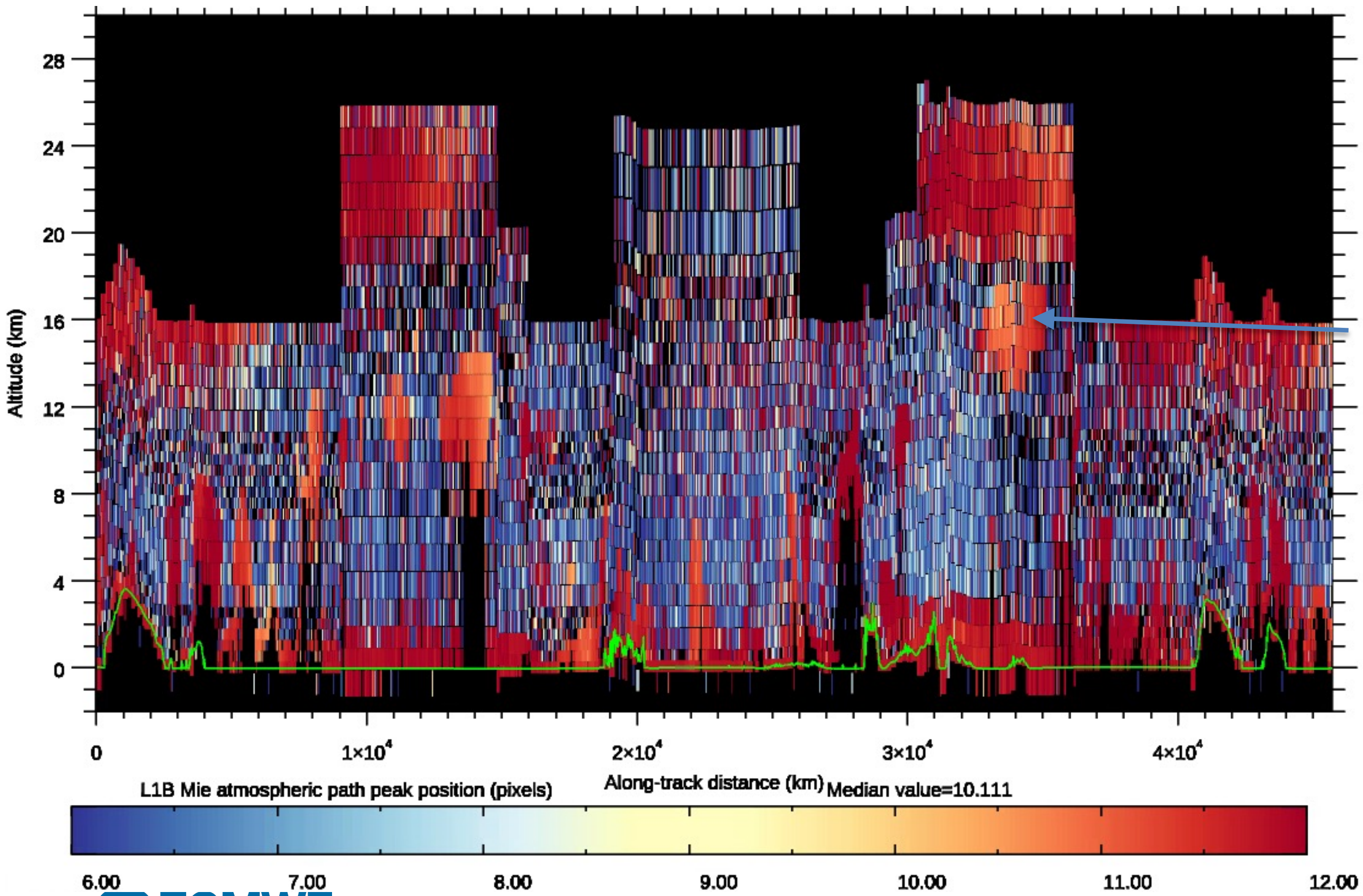


Can see variations in Mie fringe position due to horizontal wind

# Features of **D**oppler **W**ind **L**idar

- Advantages:
  - Provides Doppler shift (hence LOS wind speed) profiles
  - Good vertical and horizontal (along-track) resolution is possible
    - Complementary to relatively poor *vertical* resolution of passive sensing instruments
  - Not many processing steps and assumptions to get wind i.e. *reasonably direct measure of the geophysical variable*
- Disadvantages:
  - Totally attenuated by optically thick cloud or aerosol, need *radar* to see within clouds
  - Space-borne DWL:
    - Complicated technology
    - Several LOS "looks" are required to get vector wind, nominally have wind component along the LOS
    - Limited sampling across-track i.e. "poor swath"
    - Due to $1/R^2$ dependence of signal, then relatively *low altitude orbit* (closer to target) – hence fuel issues
  - Calibration can be tricky

# Example of Aeolus Level-2B **horizontal line-of-sight (HLOS) winds**

120 m/s polar front jet stream
9 Feb 2020; near record-breaking

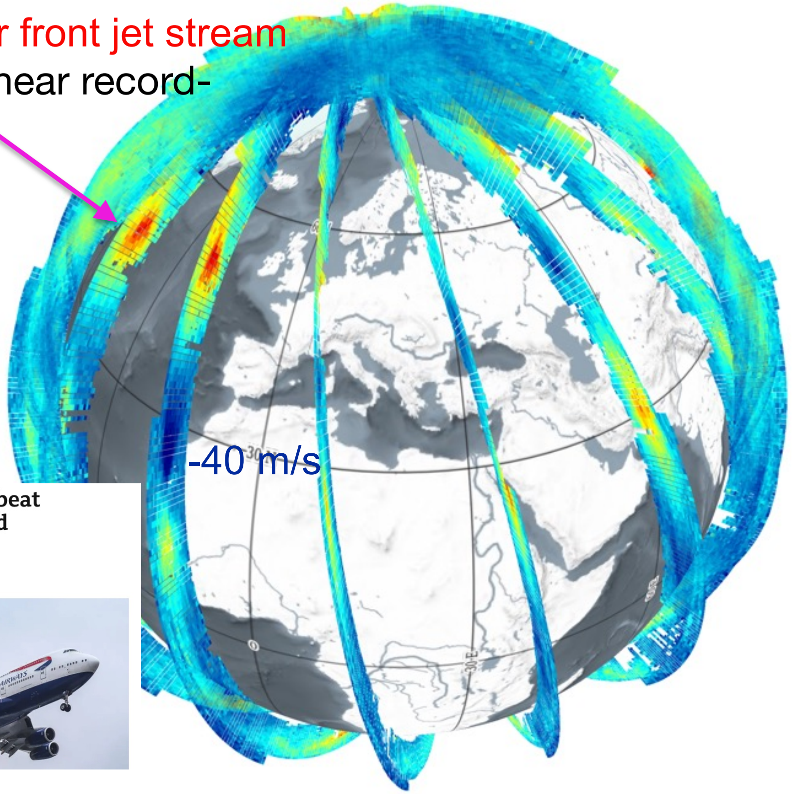



Storm Ciara helps plane beat transatlantic flight record

9 February 2020

12-hours of L2B **Rayleigh-clear** HLOS winds

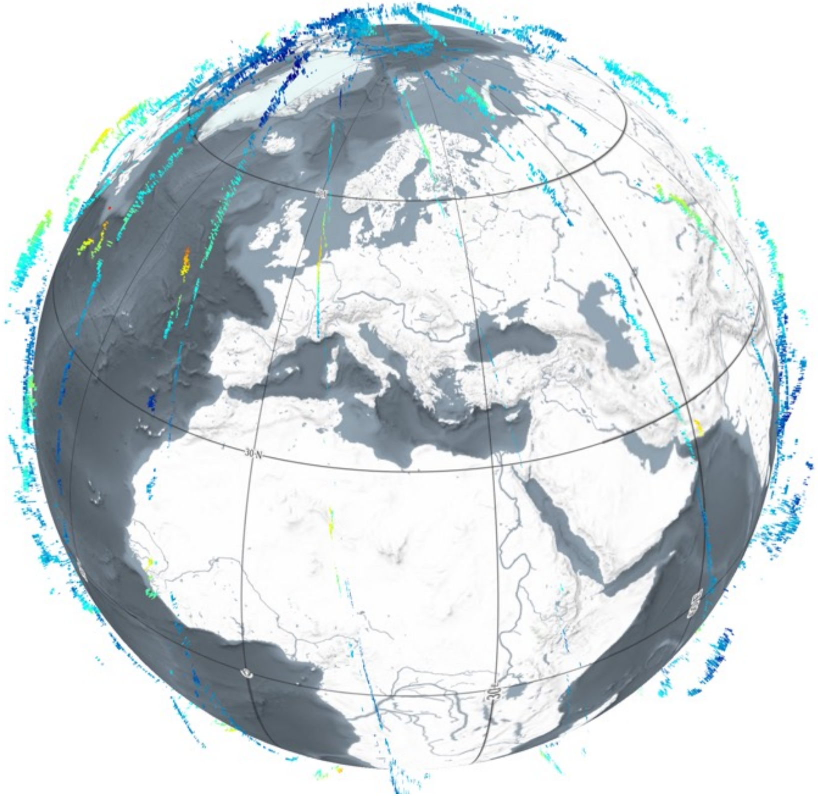

12-hours of L2B **Mie-cloudy** HLOS winds

10 Feb 2020

# Aeolus L2B Rayleigh-clear **and** Mie-cloudy HLOS winds (**1 orbit**)

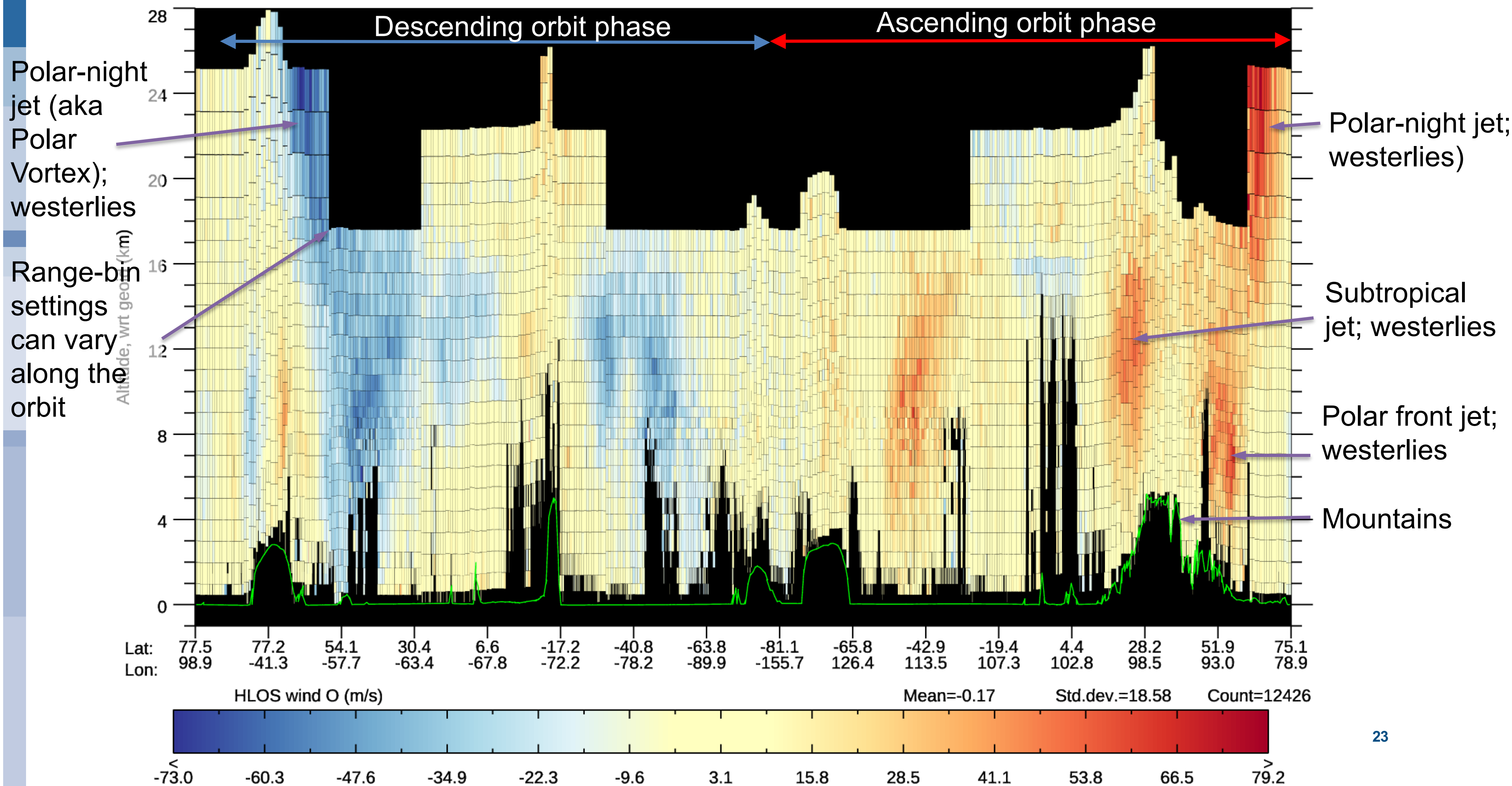

# Rayleigh and Mie winds are complementary

Mie-cloudy L2B HLOS winds

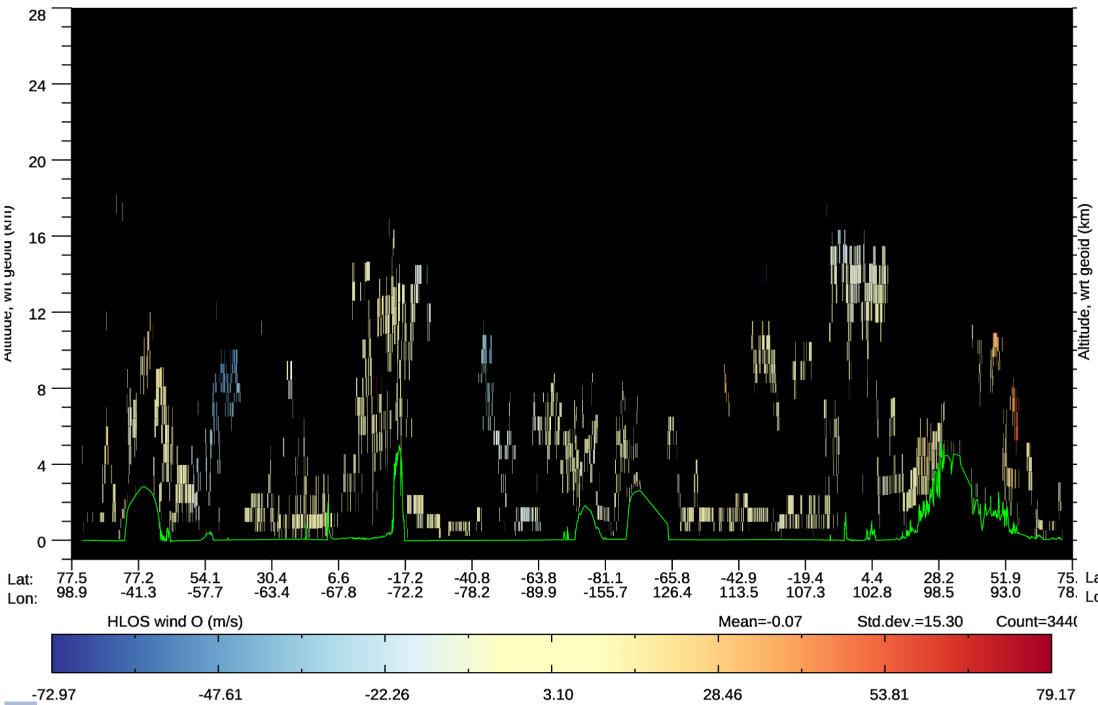


~14 km horizontal averages

Rayleigh-clear L2B HLOS winds

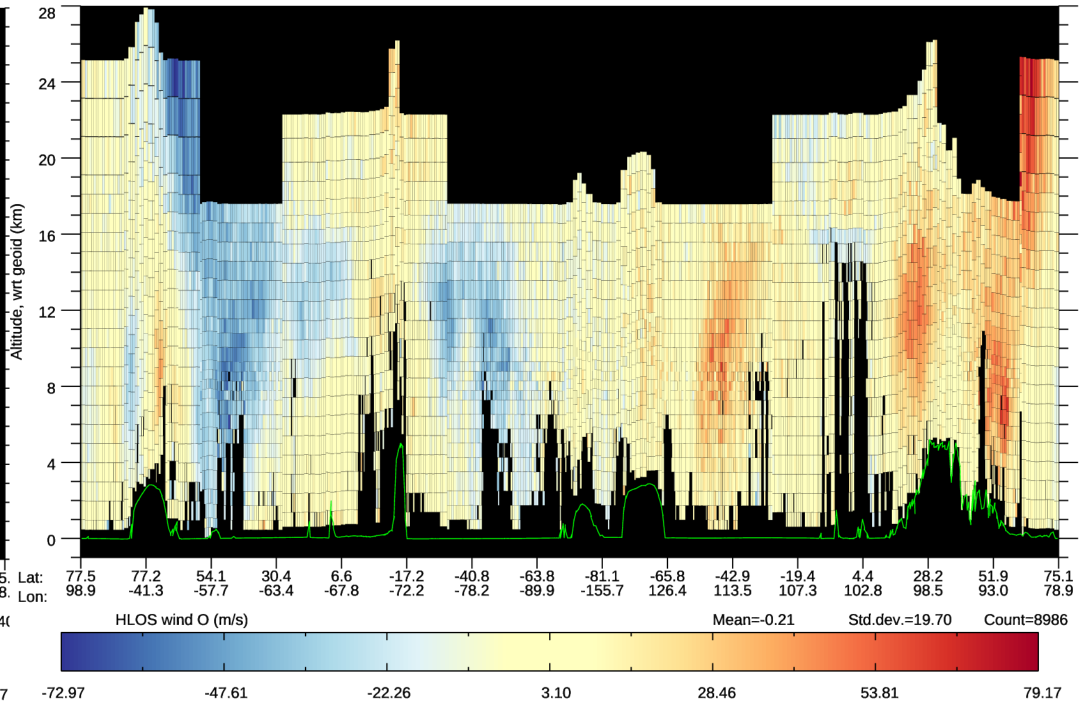


~86 km horizontal averages

ECMWF

# Use of Aeolus in NWP at ECMWF

# What to assimilate from Aeolus for NWP?

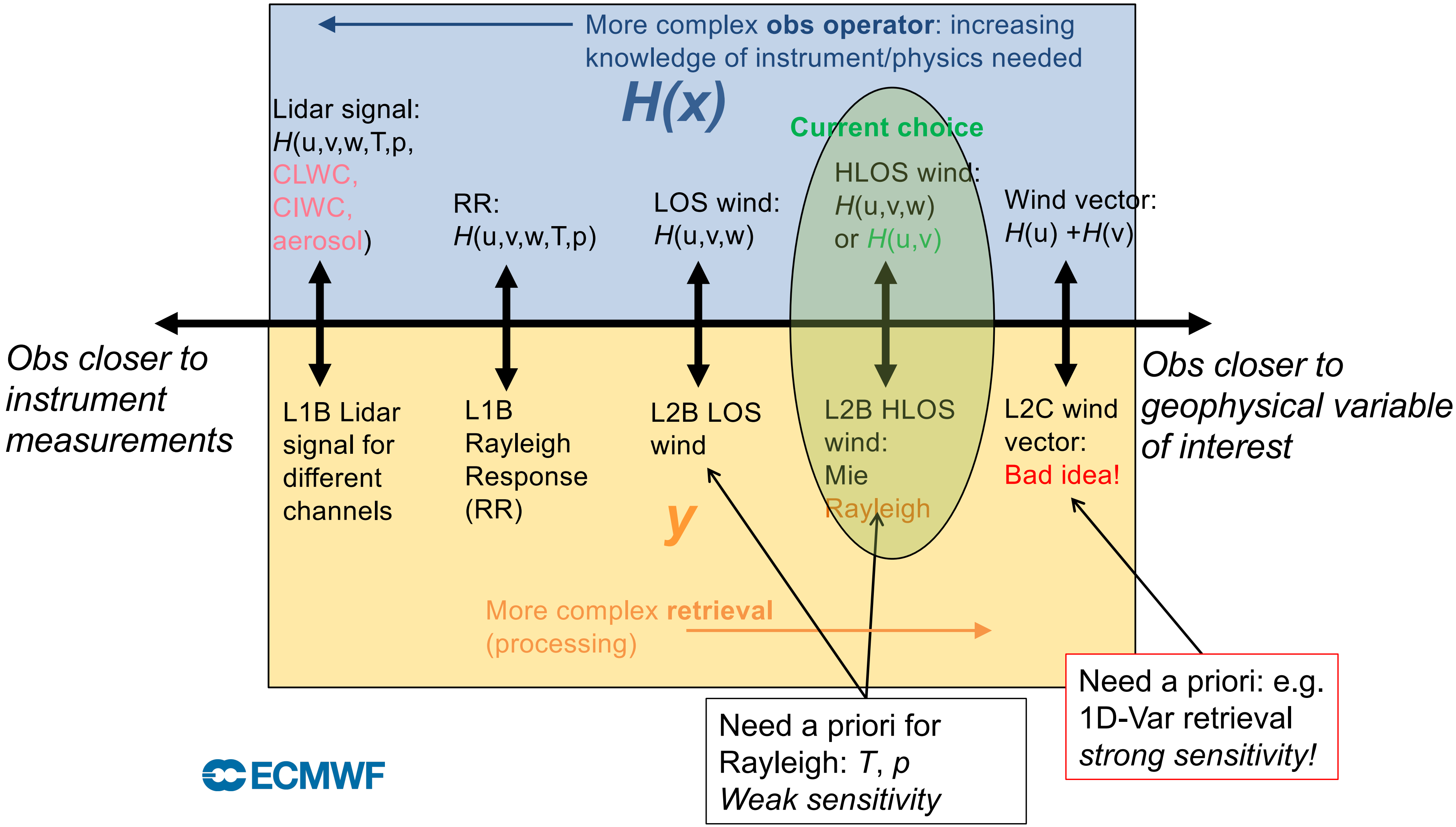


ECMWF

# L2B HLOS (horizontal line-of-sight) wind assimilation

- HLOS wind forward model
  - Interpolation of model wind to obs geolocation **point**
  - Calculate HLOS wind from model wind vector (*u*,*v*)

$$v_{HLOS} = \underline{v}.\underline{\hat{d}} = -u\sin\emptyset - v\cos\emptyset$$

∅=azimuth angle of line-of-sight

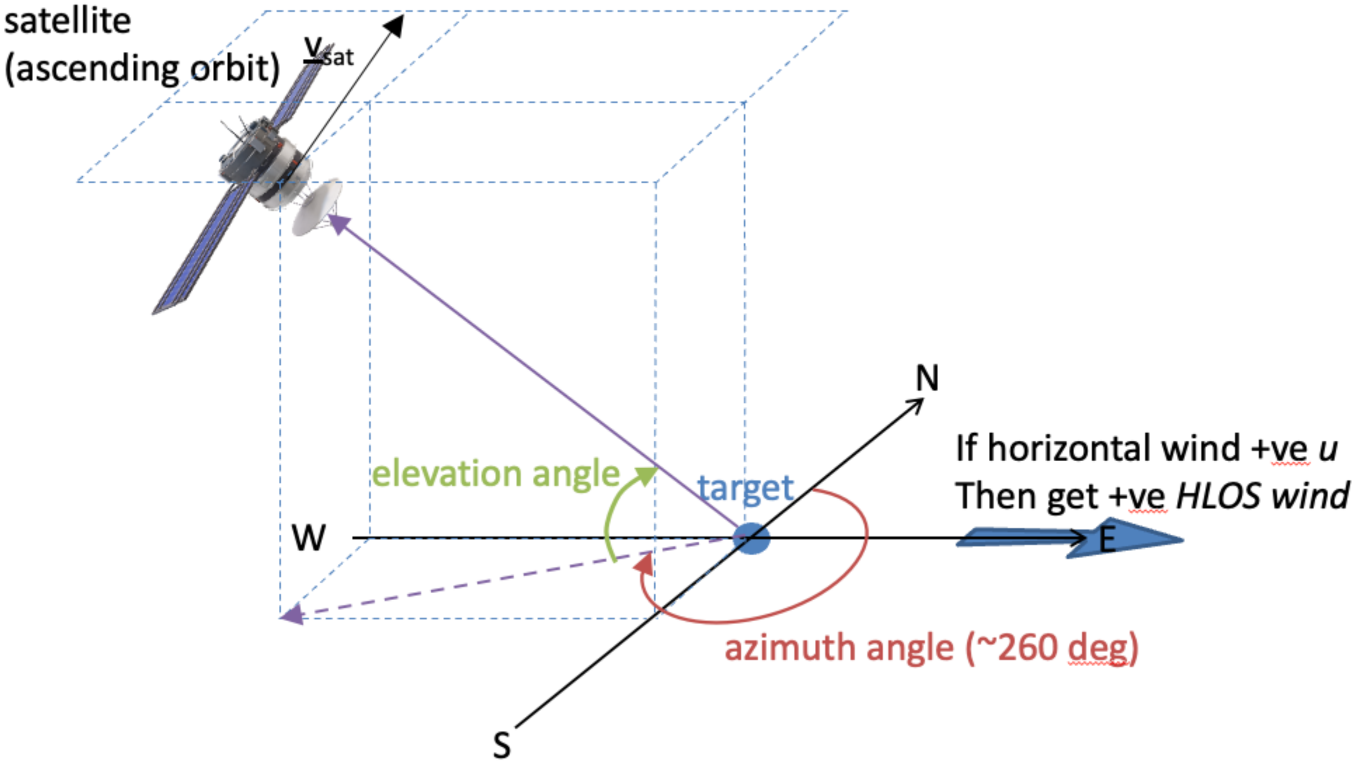


- **Assigned observation error (R matrix)** uses L2B processor **estimated instrument noise**
- Aeolus was **operationally used at ECMWF** from 9 Jan 2020 to 30 April 2023

## **ECMWF forward modelled** HLOS wind (1 orbit)

10 Feb 2020

$$v_{HLOS} = -u\sin\emptyset - v\cos\emptyset$$

*Lidar "curtain" type plot*

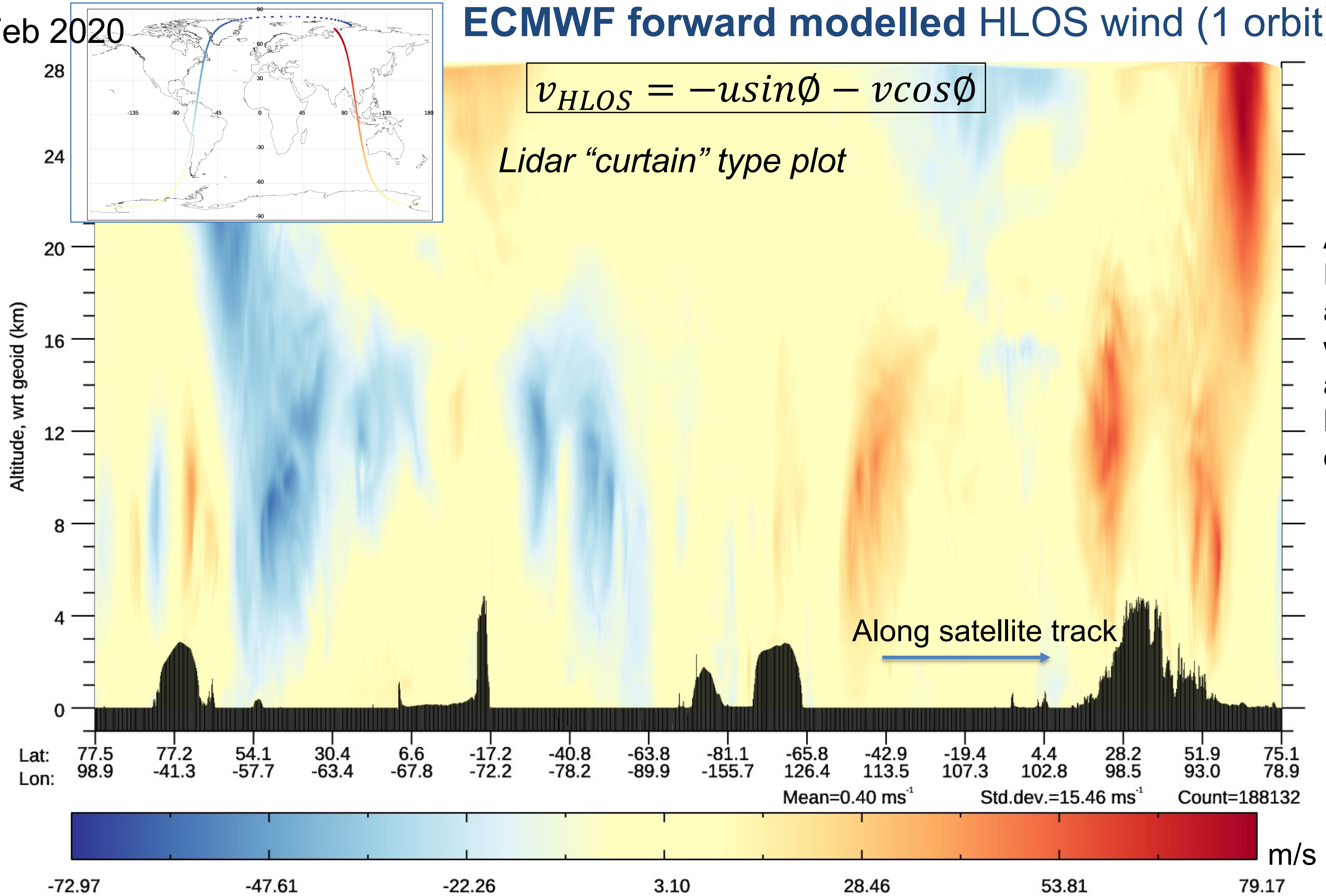


Aeolus HLOS winds are positive if wind blowing away from LOS pointing direction

# Aeolus signal levels during mission – signal dropped at steady rate for FM-A laser (first time) and FM-B. But last attempt with FM-A proved to be quite stable.

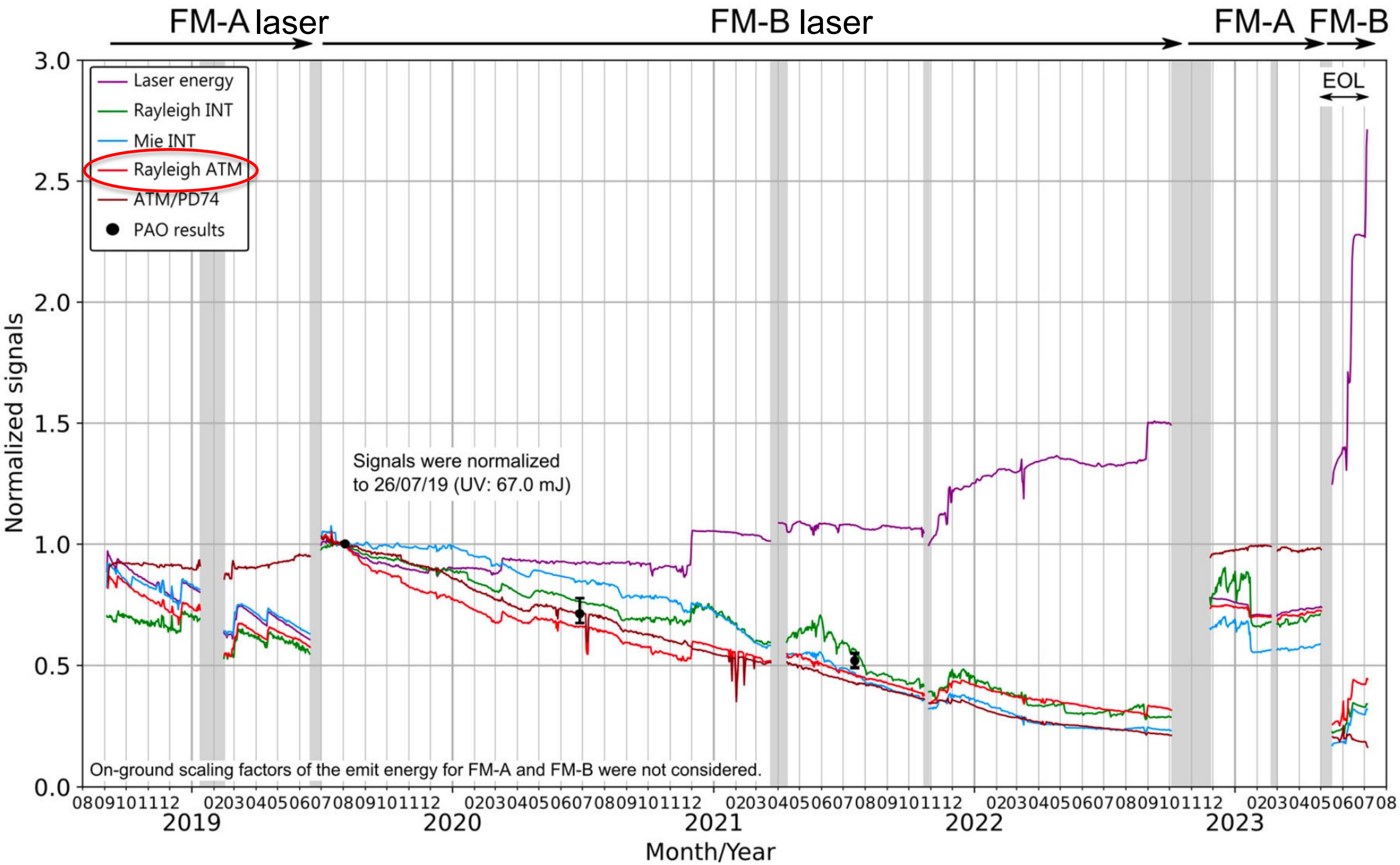


*Figure by O. Lux, DLR, Aeolus DISC*

# Global HLOS wind **O-B** departure statistics for L2B **Rayleigh-clear**, **15 July 2019 (at its best)!**

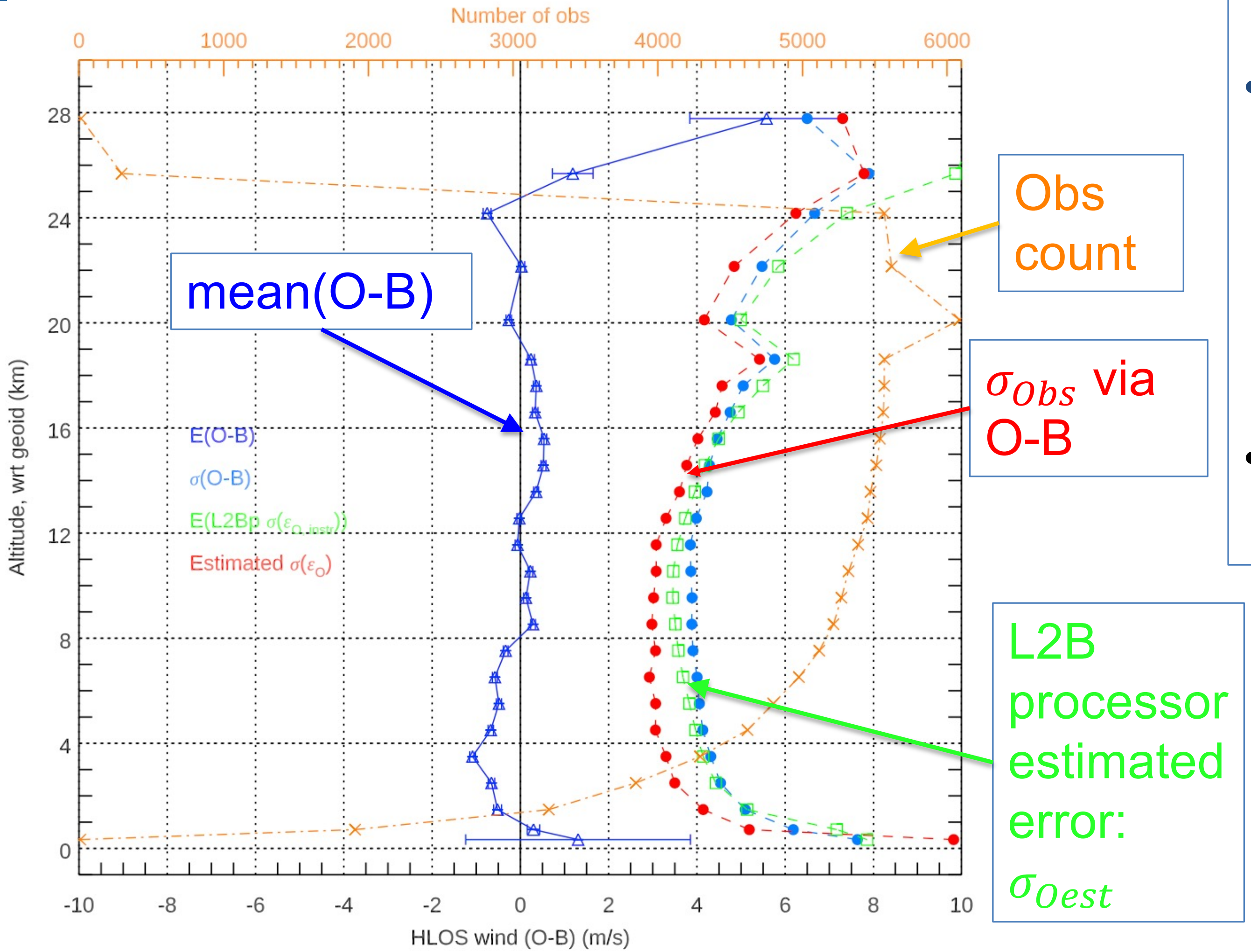


- Global average bias is reasonable
- *Estimated* observation error from O-B departures $\sqrt{st.dev.(O-B)^2 - \sigma_B{}^2}$
  - Profile average **~ 4 m/s**
  - Still larger than we hoped for before launch
- Compare: radiosonde u-wind assigned obs. error is ~2 m/s

# Global HLOS **O-B** statistics for **L2B Mie-cloudy**, **15 July 2019**

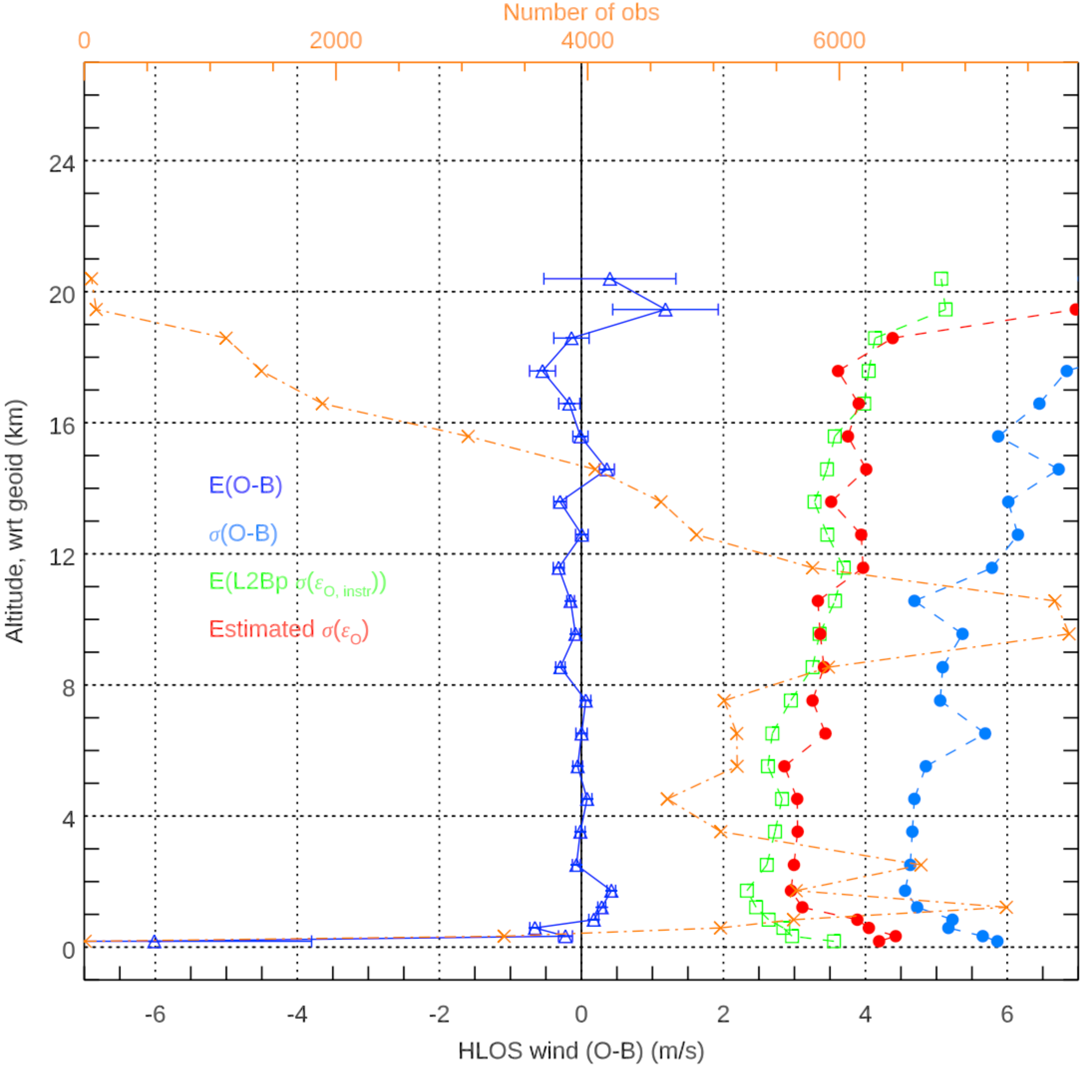


- Global average bias is reasonable and stable with time
- *Estimated* observation random error from O-B departures $\sqrt{st.dev(O-B))^2 - \sigma_B{}^2}$ is
  - Profile average **~3 m/s**
- Mie averaging length scale is ~10-20 km (Rayleigh is ≤ ~86 km)
- *Mie noise better despite finer horizontal resolution than Rayleigh*

# Aeolus Level-2B HLOS (horizontal line-of-sight) wind data quality

**Rayleigh-clear**
- Large variability of random errors (variable signal levels)
- Recent ***NRT*** FM-A laser good (best processing, reduced readout noise, reasonable signal)

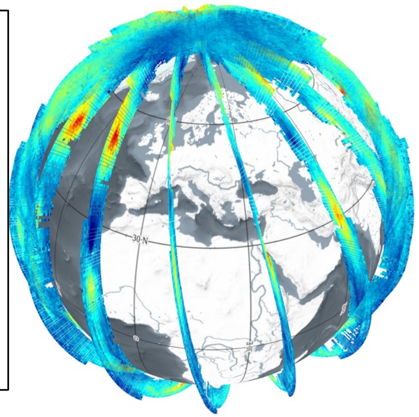

**Mie-cloudy**
- Noise **quite stable and small** compared to Rayleigh-clear
- But data count variable with signal levels/aerosol load

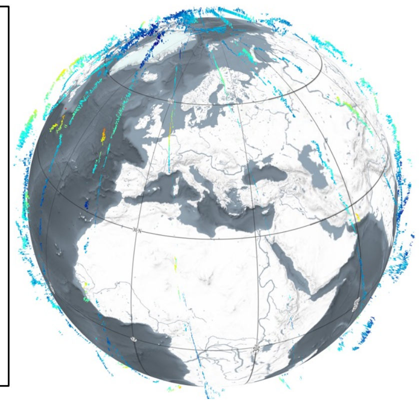

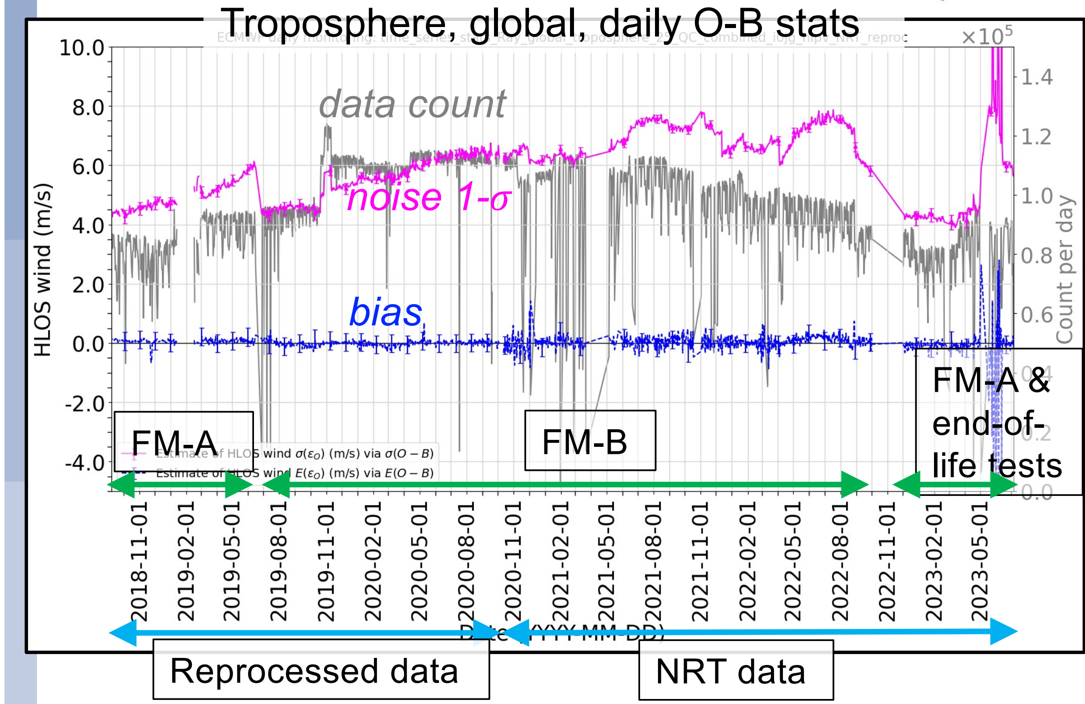


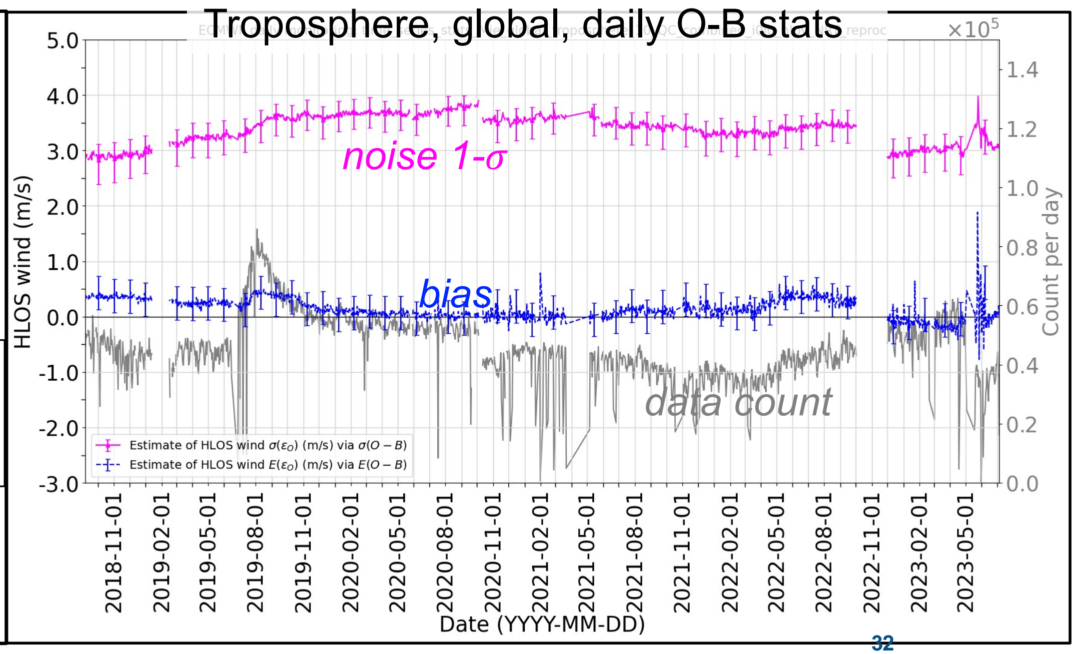

# Aeolus NWP impact at ECMWF

# Methods for Aeolus L2B wind NWP impact assessment at ECMWF

- **O**bserving **S**ystem **E**xperiments (OSEs):
  - For robust assessment of impact into the medium-range
  - 2nd reprocessed FM-B period (**OSE for long period**):
    - Rayleigh-clear + Mie-cloudy as in current operations; **29 June 2019 to 9 October 2020**
- **F**orecast **S**ensitivity **O**bservation **I**mpact (FSOI):
  - Assessment of short-range forecast impact – with some limitations
  - Operational FSOI; since 9 January 2020
  - FSOI via 2nd reprocessed dataset OSE (Aeolus "on" experiment)

Rayleigh-clear in 12 hour window

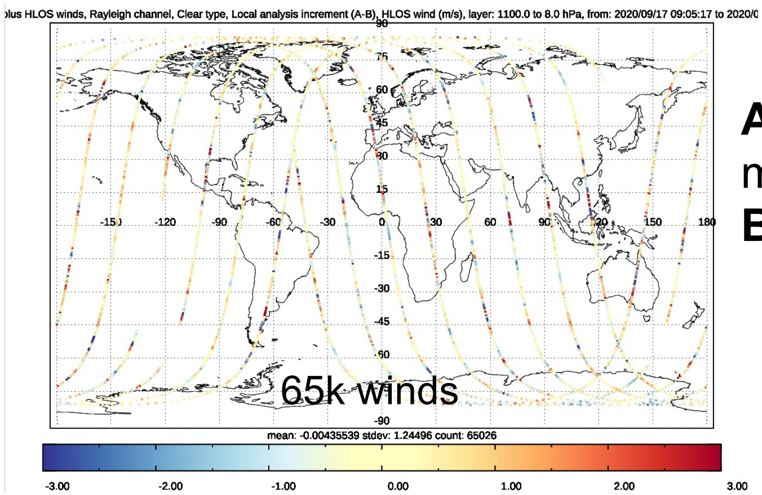


**A**nalysis
minus
**B**ackground

Mie-cloudy in 12 hour window

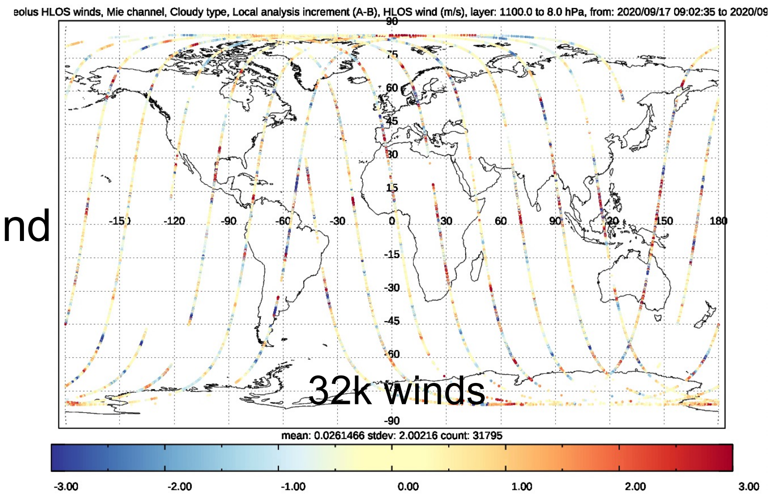

# Assimilating Aeolus winds has strong effect on zonal wind analyses

**Standard deviation of differences** in $u$ analysis

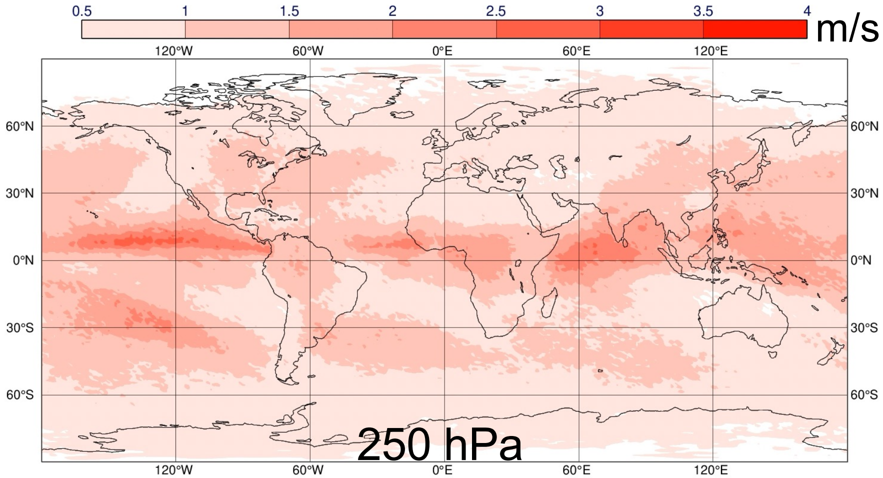


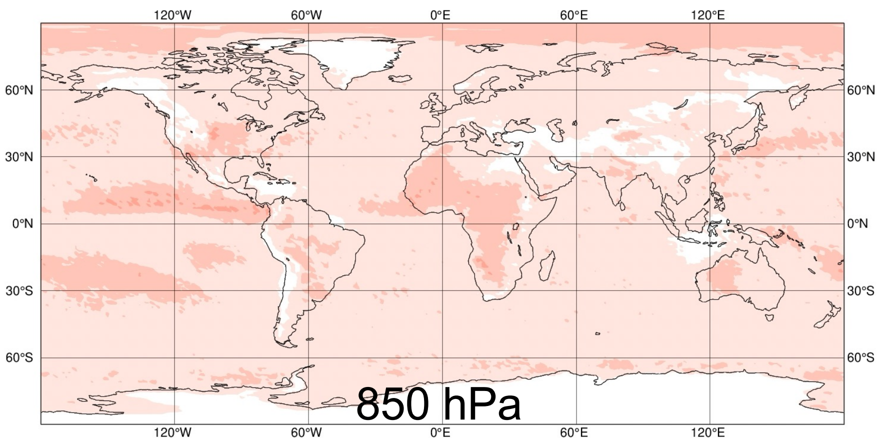


**Mean difference** in $u$ analysis at **100 hPa**

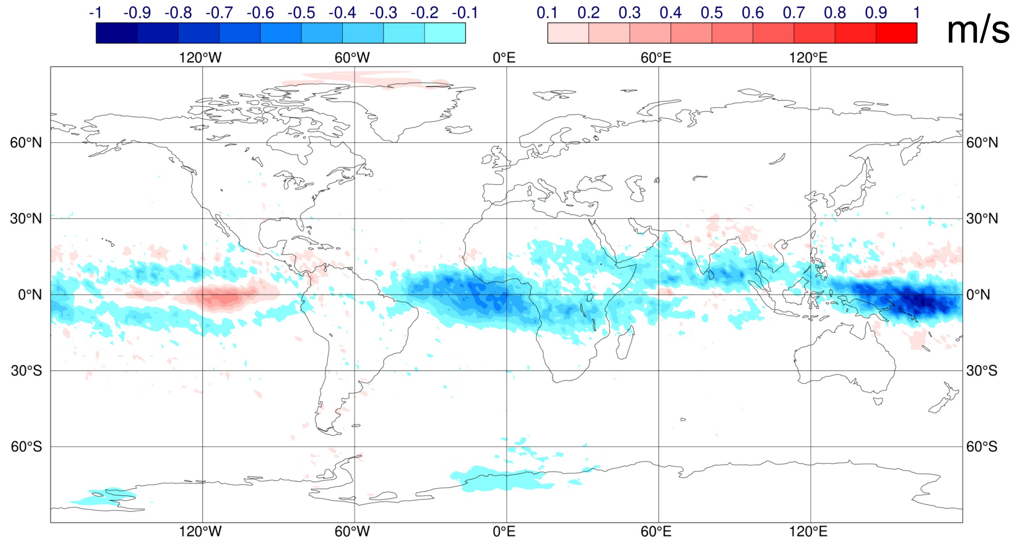


Largest changes made to tropical upper troposphere and SH extratropics – in climatological **convergence zones**; larger background wind errors associated with convection

# Independent wind observations confirm improvements from assimilating Aeolus

Fit to vector wind from aircraft, radiosondes and radar wind profilers

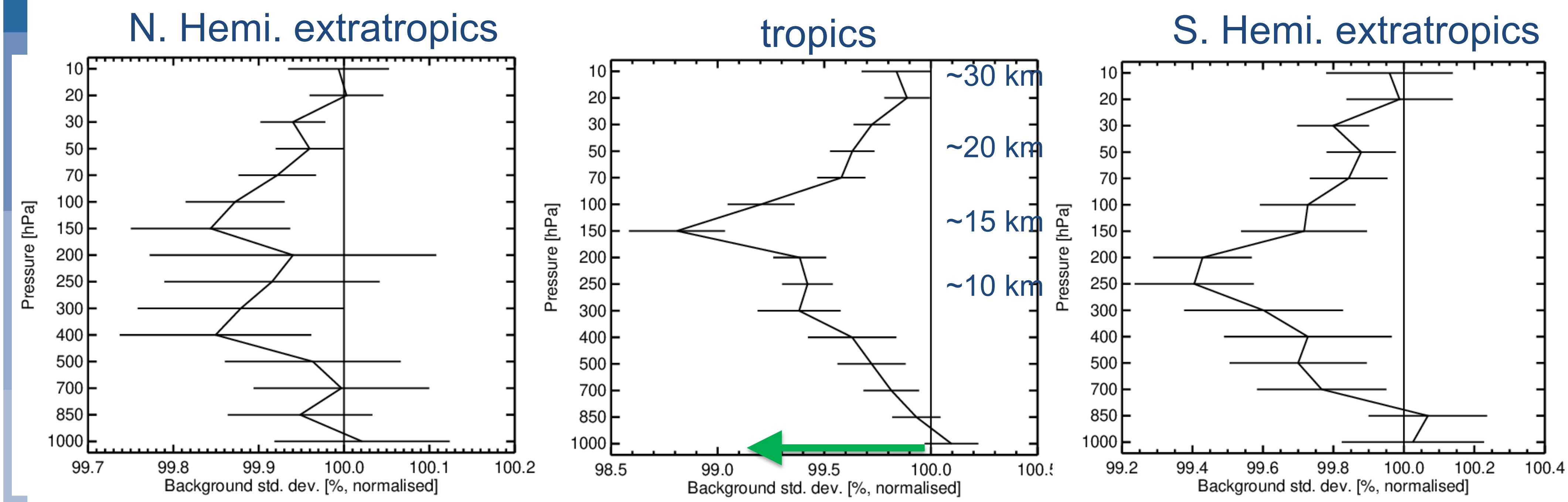


Positive impact in mid-troposphere to lower stratosphere
Largest impact on **wind in upper troposphere and lower stratosphere in tropics**

# Improved winds lead to better NWP temperature and humidity forecasts

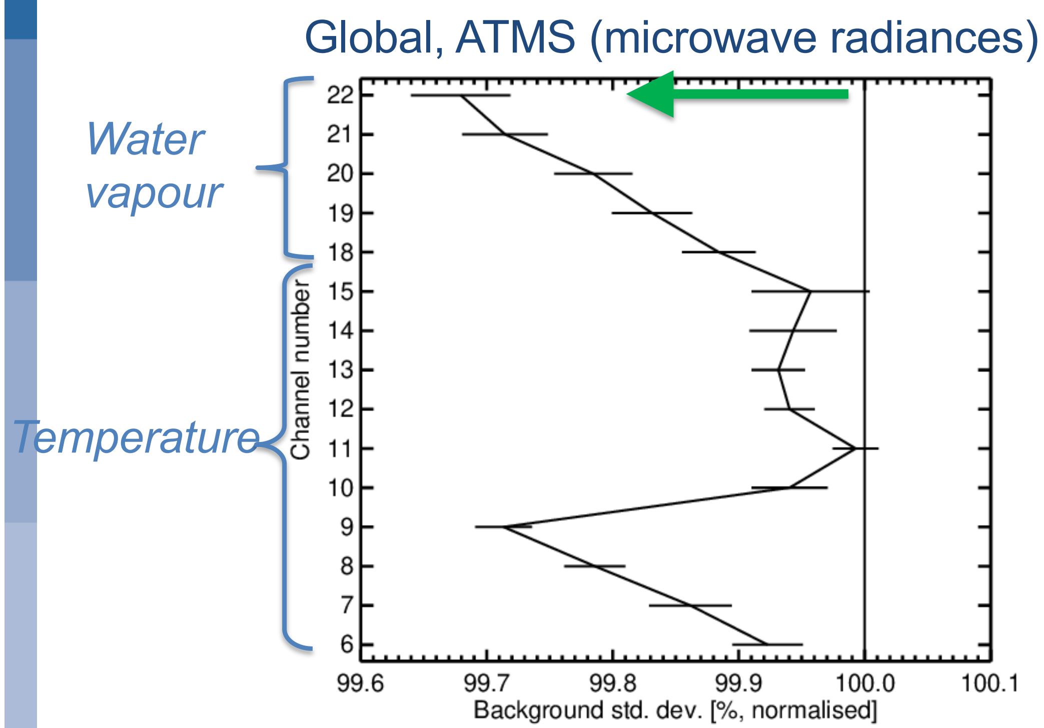


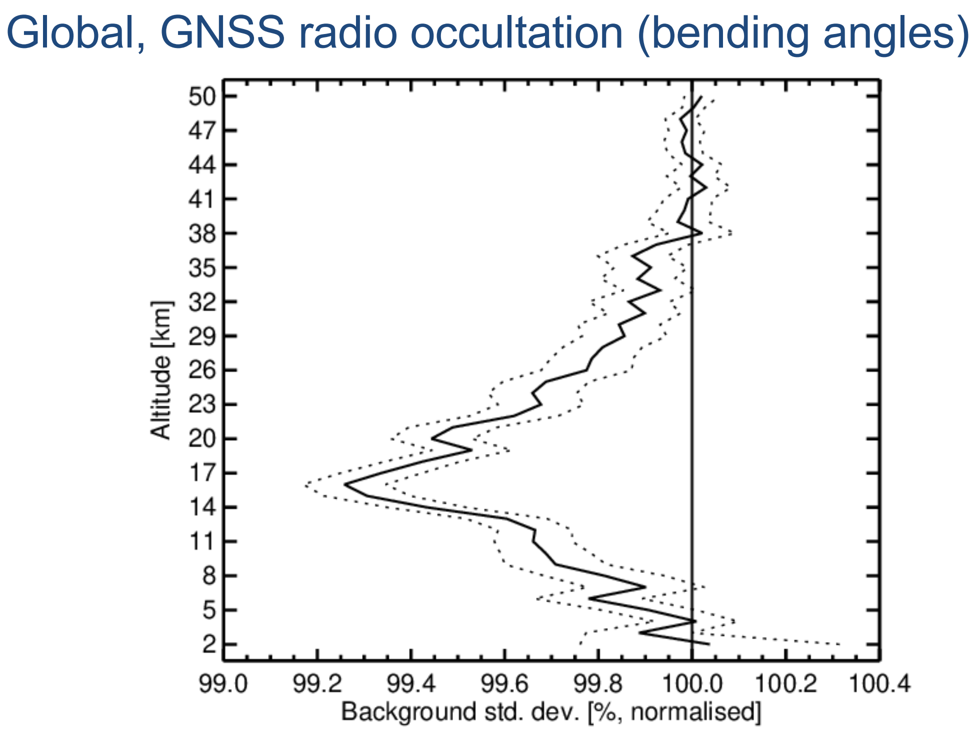


Positive impact on **temperature** and **humidity**
Strongest in **upper troposphere/lower stratosphere**

# Aeolus significantly improves NWP forecasts in most areas and forecast ranges

Vector wind RMSE zonal average

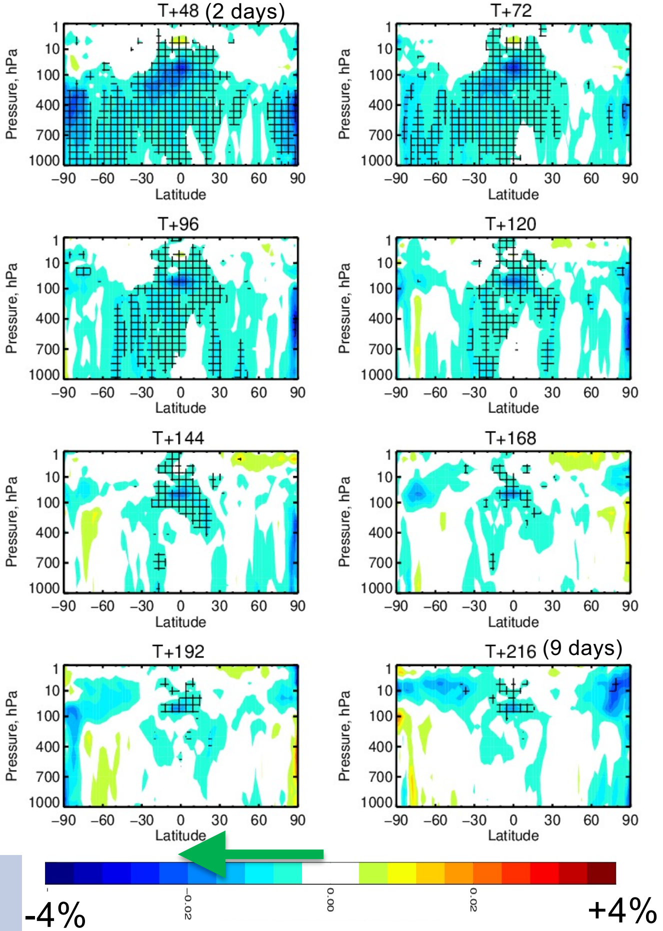


Strongest impact in tropics lower stratosphere (~20 km)

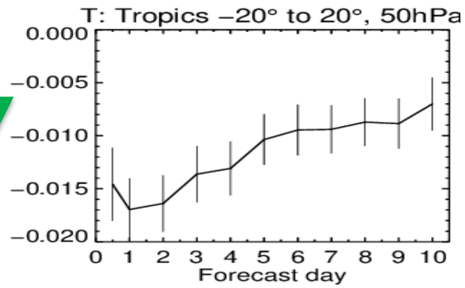


Even N Hemi. Z500 improved significant to day 4

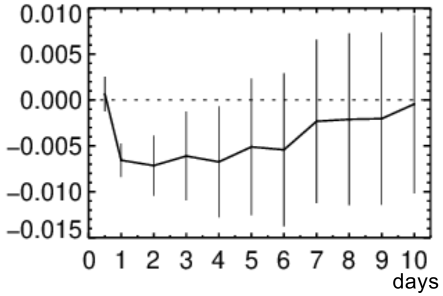


Temperature RMSE zonal average

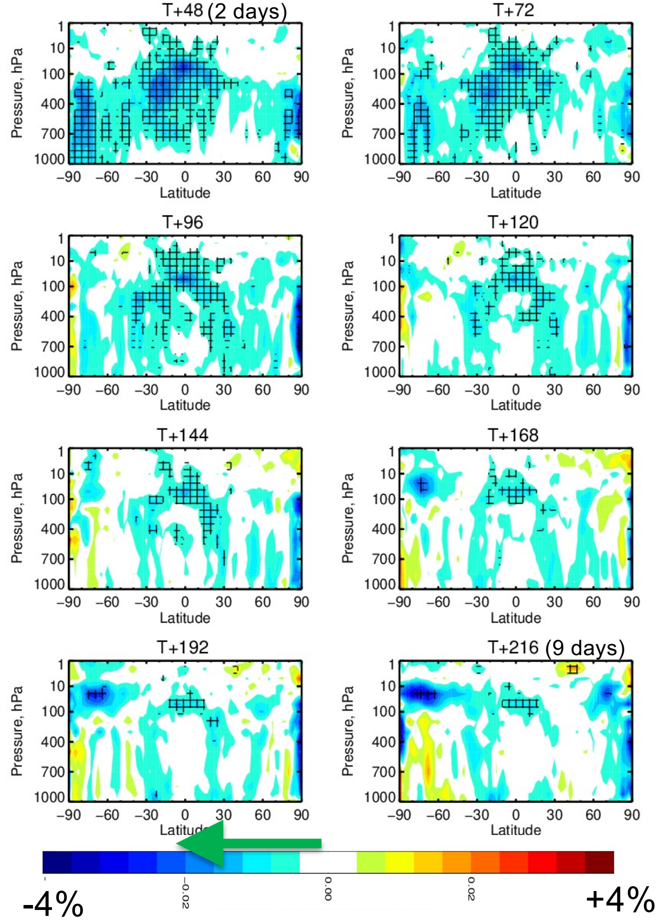


**Positive impact – good magnitude for one satellite instrument**

# Short-range forecast impact by **F**orecast **S**ensitivity to **O**bservation (FSO) time-series

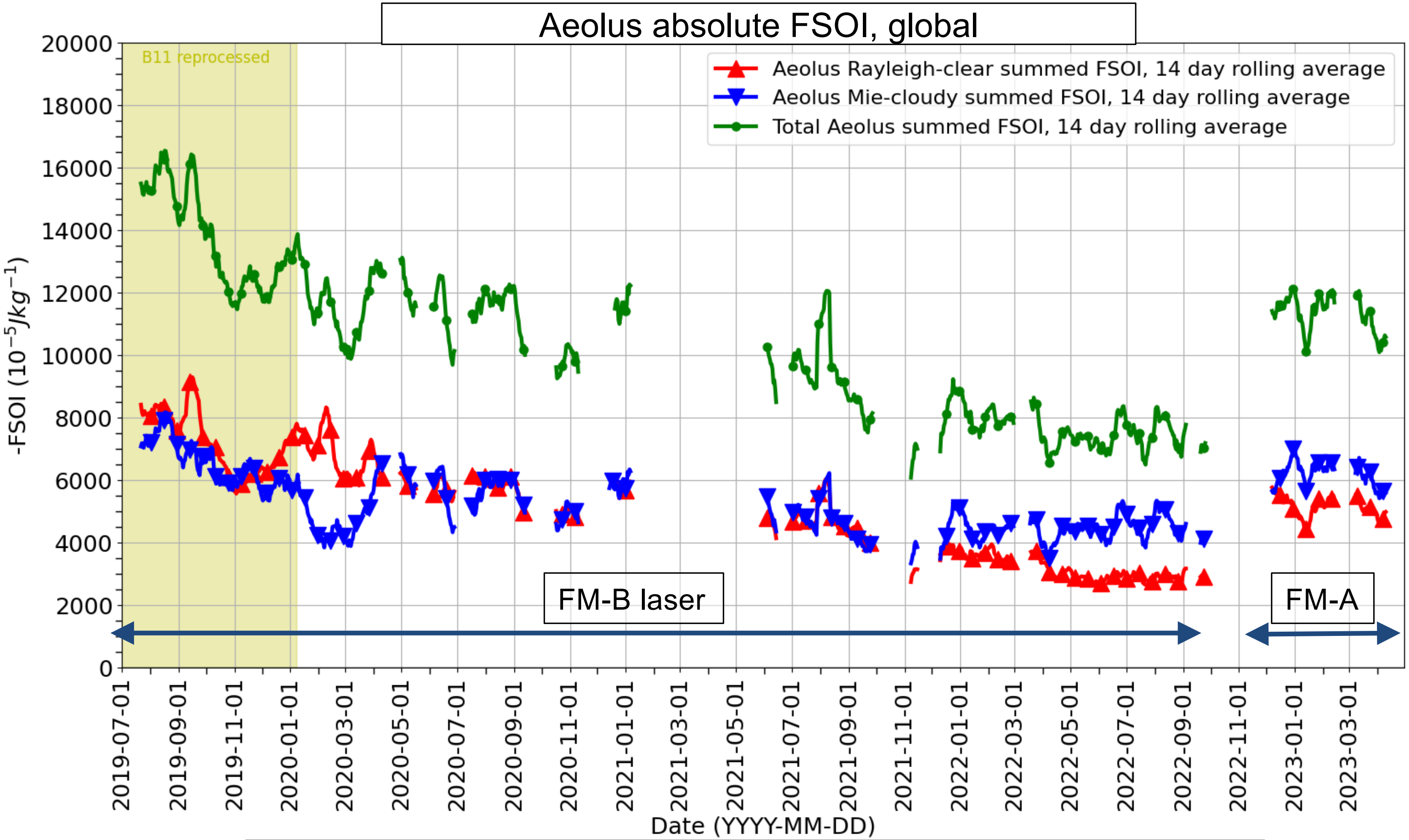


- Impact depends on random error and data counts (some gaps, QC)
- Impact was boosted by increased signal levels of FM-A in final 5 months

Impact with FM-A laser in late 2022 into 2023 increased by ~60% compared to ***end*** *of FM-B – thanks to better signal*

# Aeolus punched above its weight given the amount of data

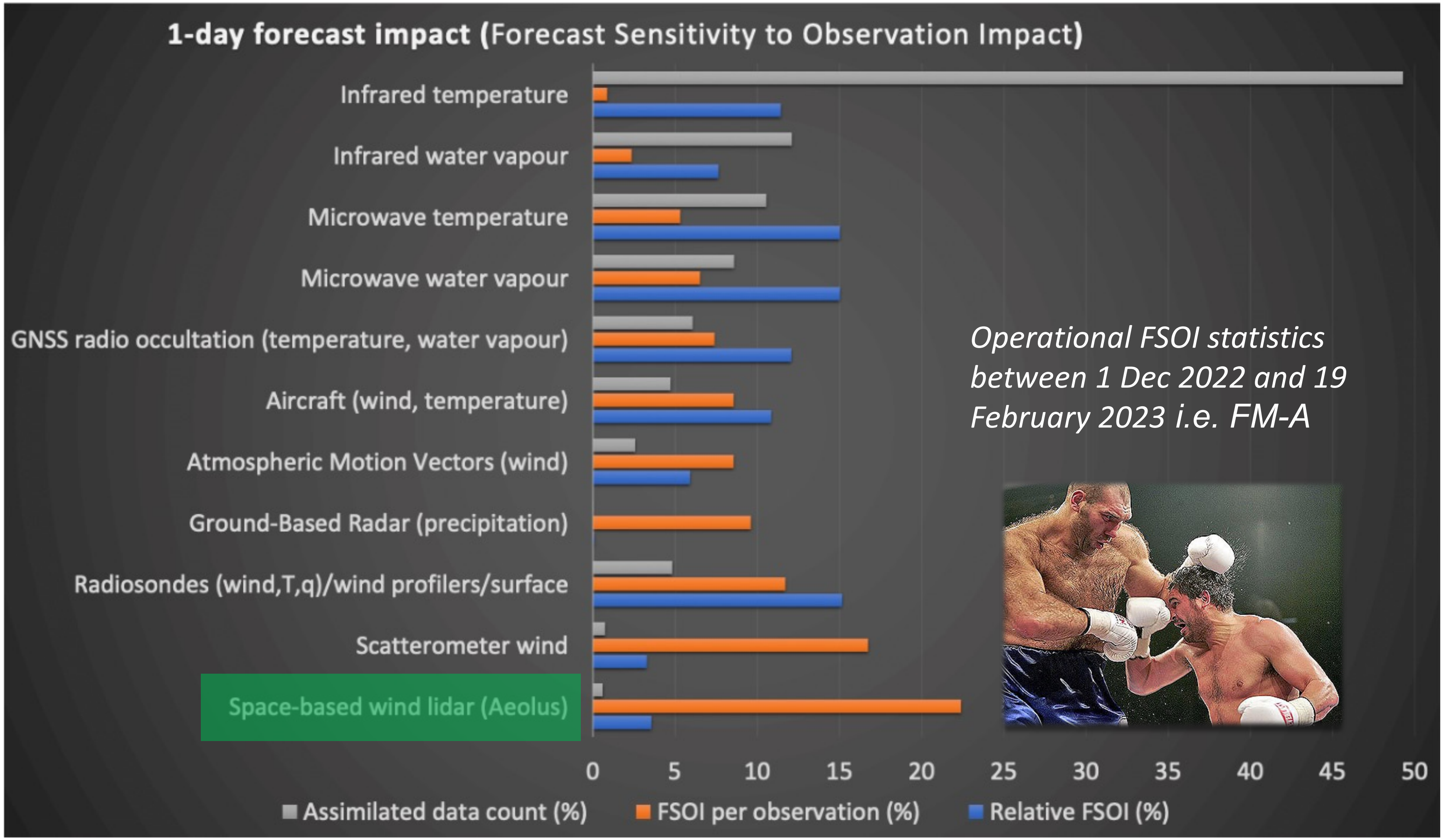

# An impression of analysis u-component wind **random errors**: stdev of **ECMWF minus Met Office** analysis differences: 1 Jan to 20 Feb 2023

500 hPa

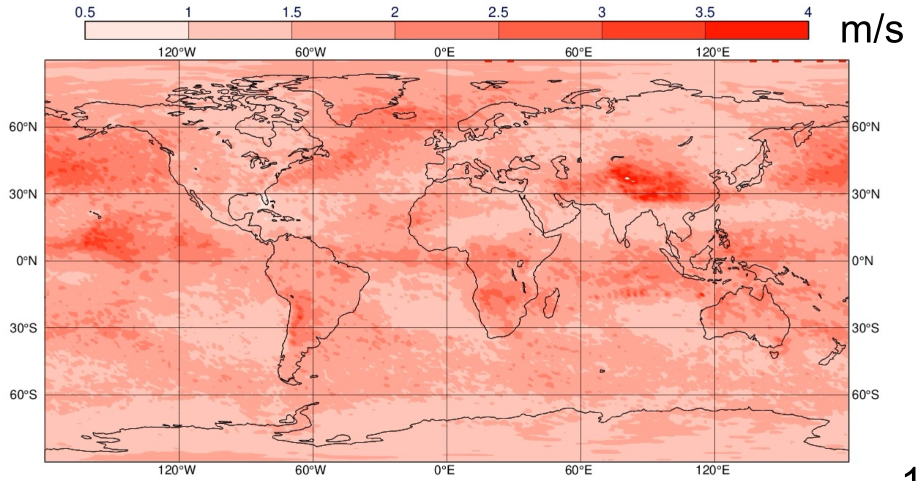


250 hPa

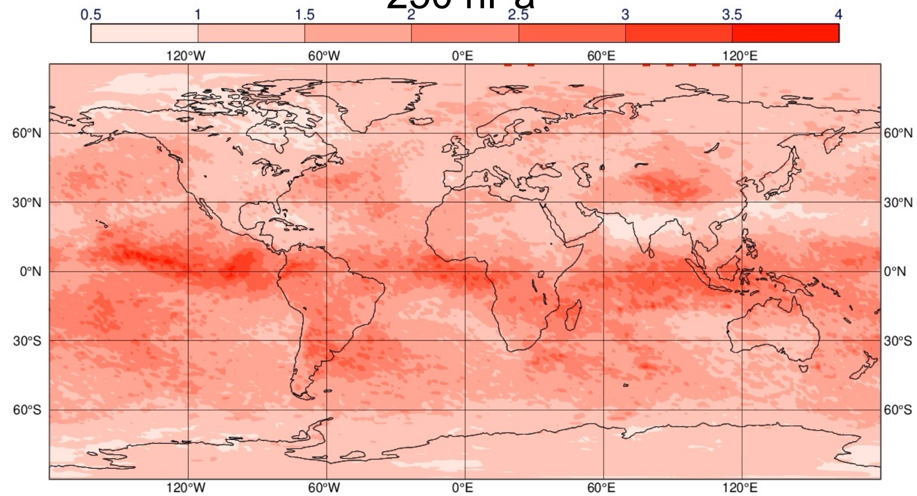


100 hPa

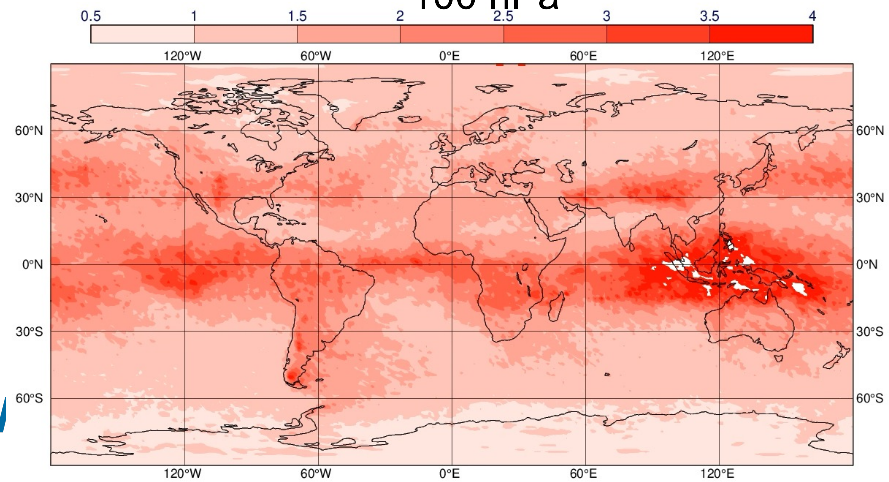


NWP *analyses* of wind are quite uncertain in tropics/oceans; **random errors** ~3 m/s

Can estimate $1\sigma$ of u-error of ECMWF analysis, by multiplying by $\frac{1}{\sqrt{2}}$~0.7 (assuming similar random error for ECMWF and MO)

# An impression of analysis u-component wind **systematic errors**: mean of **ECMWF minus Met Office** analysis differences: 1 Jan to 20 Feb 2023

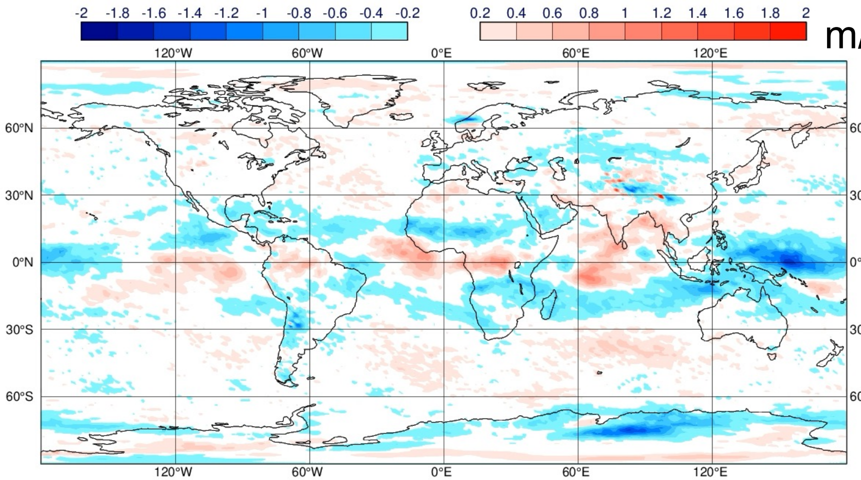


m/s

500 hPa

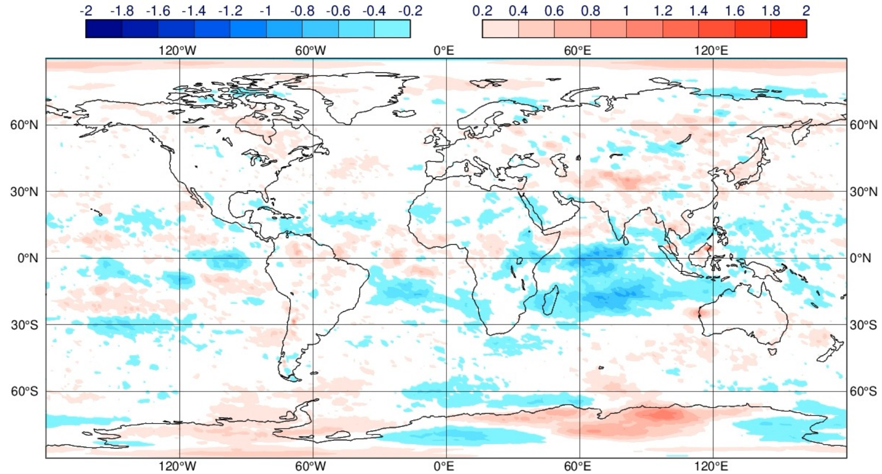


250 hPa

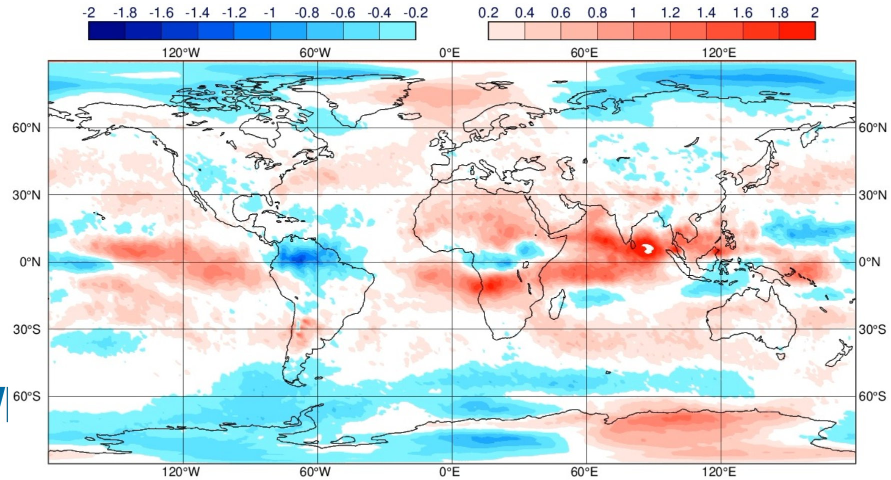


100 hPa

NWP *analyses* of wind are quite uncertain in tropics/oceans; **biases** of 1-2 m/s

## Some other demonstrated benefits in atmospheric sciences from Aeolus

- Applications in *atmospheric dynamics* research:
  - gravity waves, equatorial waves, SSW events, QBO monitoring – improving understanding of Earth's climate

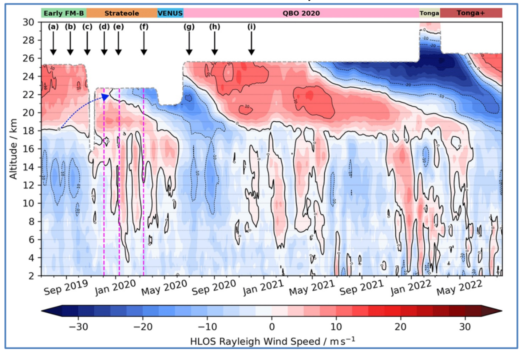


e.g. https://doi.org/10.5194/acp-24-2465-2024

- Optical properties for *atmospheric composition* research:
  - Wildfire smoke, Saharan dust, volcanic eruption plumes, atmospheric composition data assimilation
  - Unique ability of Aeolus to **measure dynamics and optical properties** should be exploited further – coupled composition and dynamics forecasts
  - **Cloud** properties. *Mark Fielding (ECMWF) has been testing assimilating cloud information from Aeolus*

- Aeolus winds are useful for verifying/improving usage of other satellite wind observation types e.g. **A**tmospheric **M**otion **V**ectors and checking if other observation types are improving wind

# Summary on Wind Information from Aeolus

- Novel **space-based** technology is required to **actively sense wind** profiles – Aeolus Doppler Wind Lidar demonstrated this
- Measured signals have a reasonably **direct link** to **wind** geophysical variable
- Positive NWP impact corroborates dynamical reasoning on **importance of global, vertically resolved wind** profiles
- Applications in atmospheric **clouds, dynamics** and **composition** research

- **In upcoming years:**
  - Focus on achieving best quality reprocessed datasets for research and reanalysis (ERA6) and maximising impact
  - **Operational follow-on mission (EPS-Aeolus)** with two satellites (one after other) in 2031 time-frame is being prepared by ESA/EUMETSAT – *decision on "programme" by EUMETSAT member states in 2025*
    - *Many improvements planned relative to Aeolus – so increased impact*

Thanks for listening. Any questions?

# Backup slides

# Aeolus' orbital parameters

Aeolus track in July

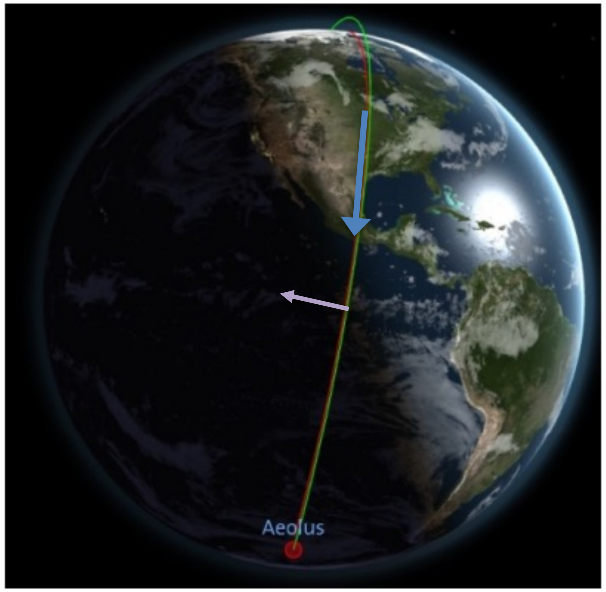


Aeolus track in October

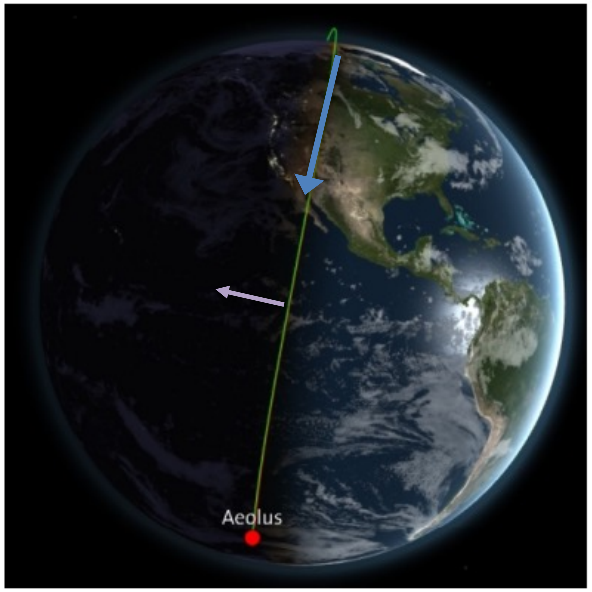


- Dawn-dusk sun synchronous (18:00 ascending node)
- 7 day repeat cycle (111 orbits)
- Inclination: ~97 degrees
- Altitude: ~320 km
- The laser points towards the dark side of the terminator to reduce UV solar background noise – but this can't be avoided over the poles in summer

# Types of Doppler wind lidar

- Coherent detection
  - Detecting beat signal mixing of returned signal with internal reference
  - Particulate (Mie) scattering only
- **Direct detection:**
  - Aeolus uses this
  - Measurement is *signal intensity* (or *photon counts)* through optical filters (interferometers) which varies with the frequency of light
  - Molecules *and* particles are the source of the backscattered signal
    - Useful for NWP to have both clear air + cloud/aerosol winds

# Aeolus Rayleigh channel

Uses “filter method”, specifically the double-edge technique

- Two frequency filters (A and B) sample sides of Rayleigh-Brillouin spectrum, providing photon counts
- Contrast function (response) calculated from counts: $\boldsymbol{R} = \frac{\boldsymbol{A}-\boldsymbol{B}}{\boldsymbol{A}+\boldsymbol{B}}$
- *R* is measured for both internal reference (i.e. outgoing laser spectrum) and for atmospheric return
- Calibration is needed for both internal and atmospheric responses to relate response to frequency
- Change in frequency of atmospheric relative to internal frequency is obtained $\Delta \boldsymbol{f} = \boldsymbol{f}_{\boldsymbol{atm}} - \boldsymbol{f}_{\boldsymbol{int}}$ i.e. the Doppler shift, hence LOS wind

# Aeolus Mie channel

Wind derived from the narrow Mie spectrum obtained by "Fringe Imaging Technique"

- Position of interference pattern (called a "fringe") is related to frequency (by calibration), both for the internal and atmospheric returns
- Measured fringe centroid for both internal and atmospheric signals is then converted to frequency, hence calculate $\Delta \boldsymbol{f} = \boldsymbol{f}_{atm} - \boldsymbol{f}_{int}$ i.e. the Doppler shift, hence LOS wind

## How Aeolus products were produced in NRT

Wind products were produced in NRT for the benefit of operational NWP – *despite being only a demonstration mission*

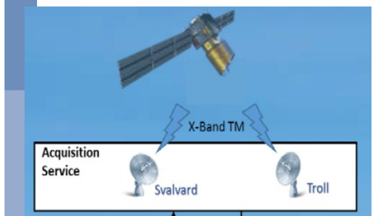


Raw satellite telemetry

L0 and L1A data

ESA-ESRIN produce **Level-1B** data (calibrated signal levels)

L1B

**Level-2B** wind product (aimed at NWP); produced by **ECMWF**

L2B

ECWMF data assimilation analysis

L2C

L2B BUFR files from ECMWF sent to EUMETSAT for distribution on GTS/EUMETCast

L2A

ESA-ESRIN produce L2A (optical properties) product

**L2B processing** algorithms developed mostly by KNMI, ECMWF, Météo-France, DLR and DoRIT

# There are 24 vertical range-bins to assign

- Range-bin thickness can vary from 0.25 to 2 km thick in 0.25 km increments
- Rayleigh and Mie range-bin settings can be different
- Range-bins settings can vary according to latitude/longitude boxes that are defined on-board the satellite
  - An attempt has been made to optimise the settings for NWP impact – varying with latitude

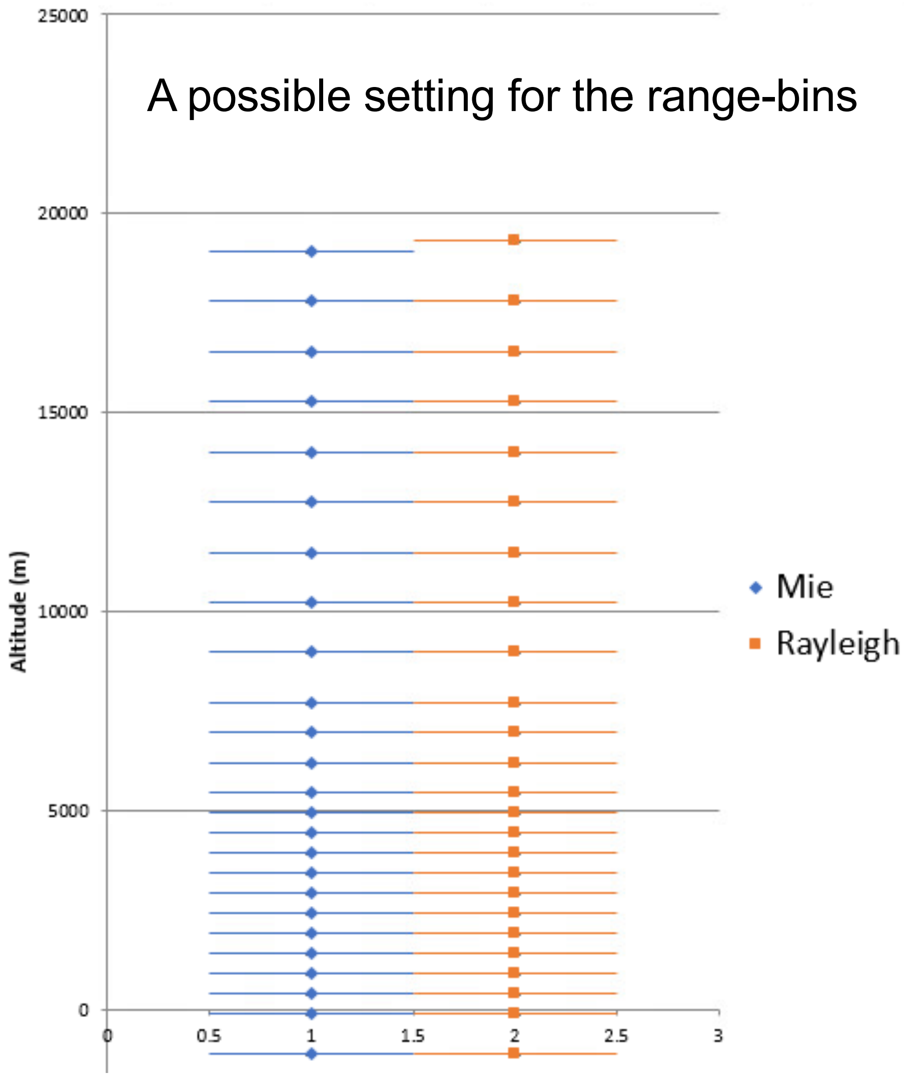

# Aeolus Payload Data Ground Segment

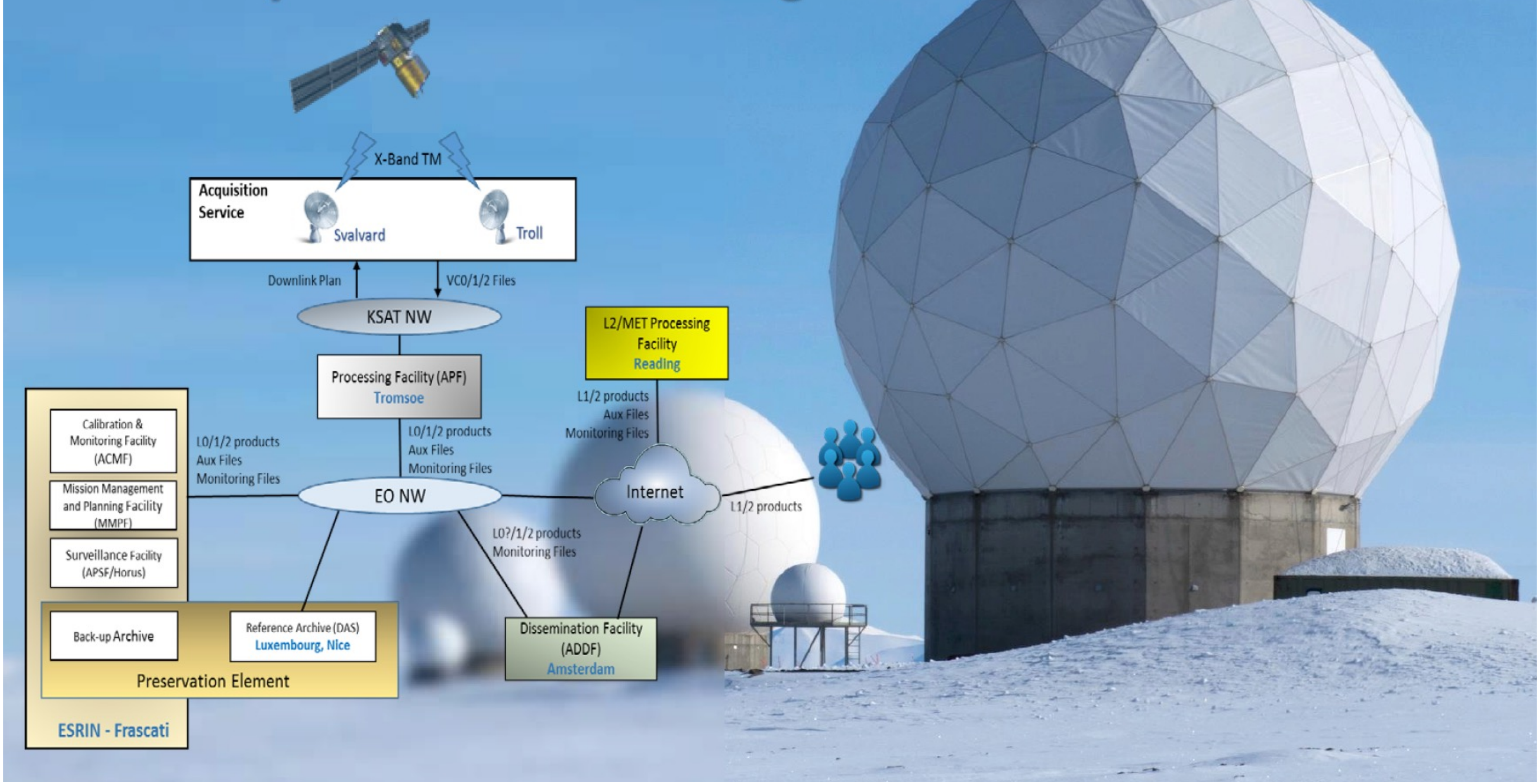

# Example of Level-1B signal amplitude (photon counts, i.e. *not winds)* for a 3000 km stretch of data

Each data point is ~2.7 km across (a flexible instrument setting)

Rayleigh channel signal

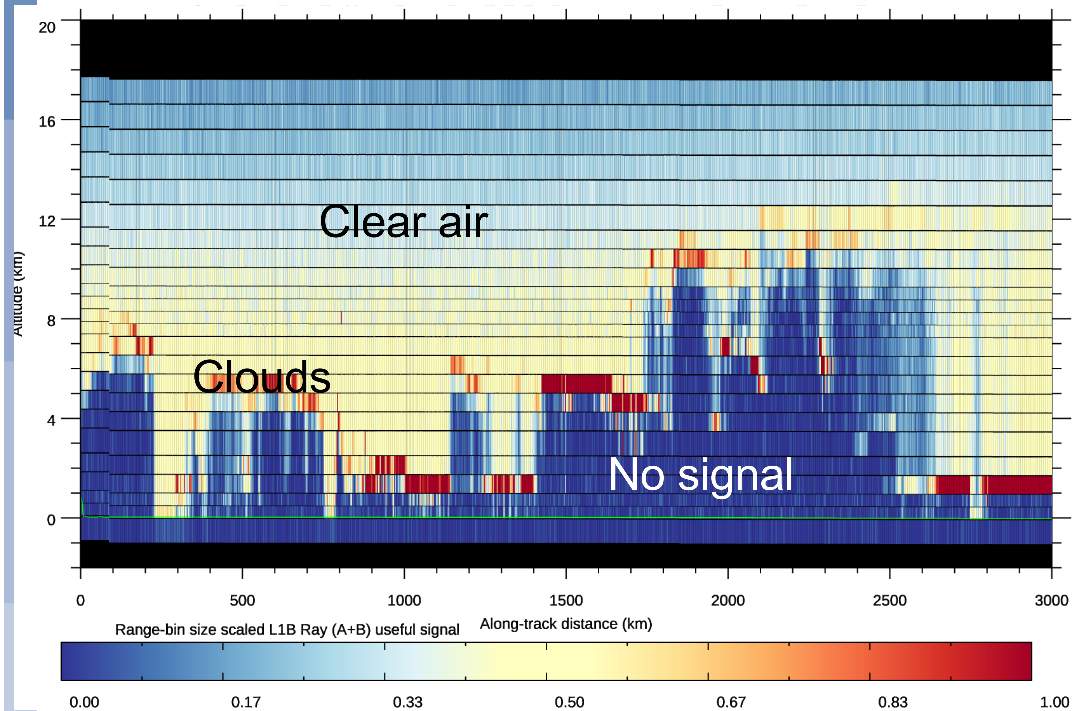


Mie channel signal

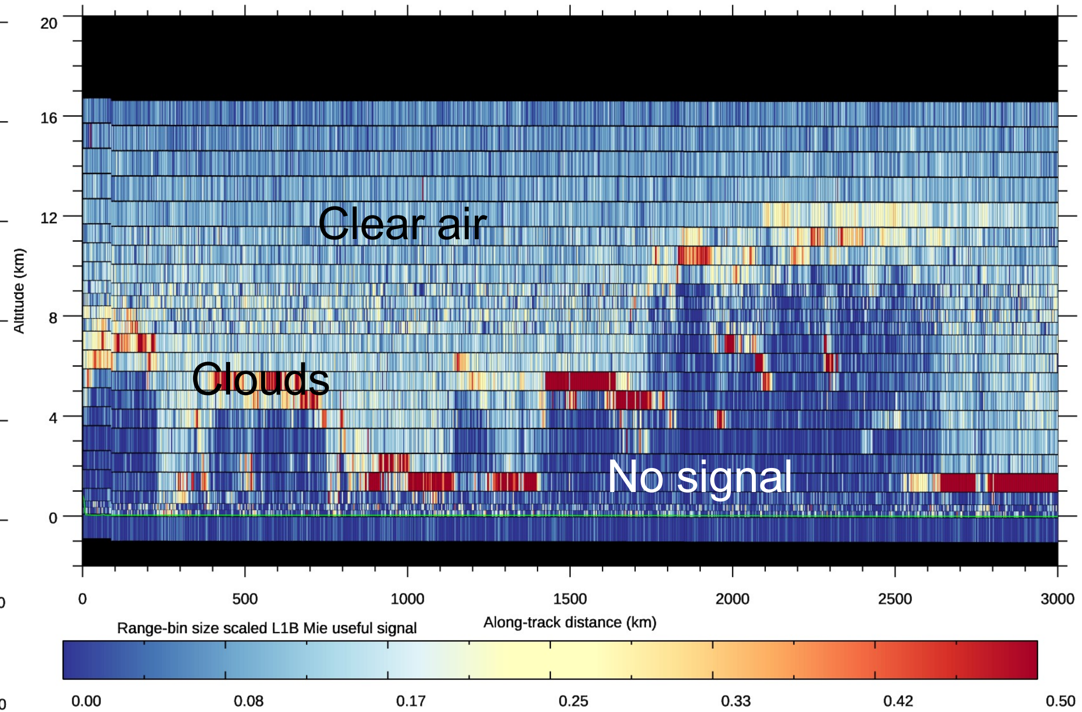


ECMWF

Satellite moves at ~7.3 km/s to sweep out this lidar "curtain"

# Real Aeolus measurement signal amplitudes

## Aeolus L1B signal levels on Rayleigh channel

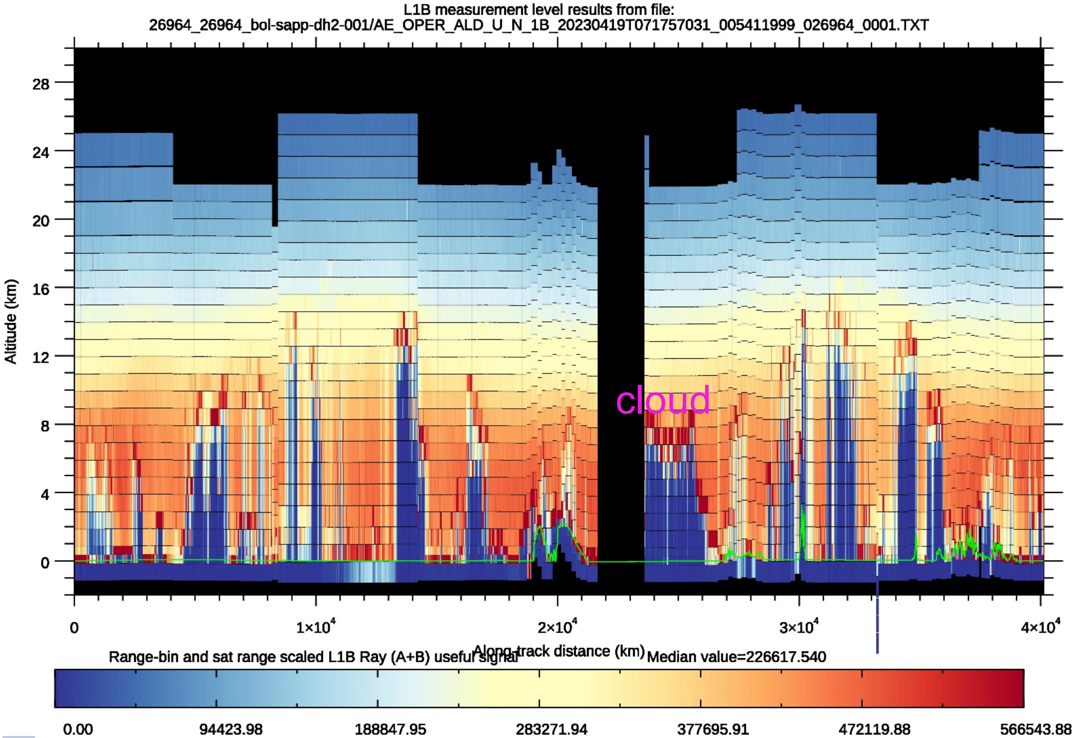


24 vertical range-bins are evident

## ECMWF “forward modelled” attenuated backscatter

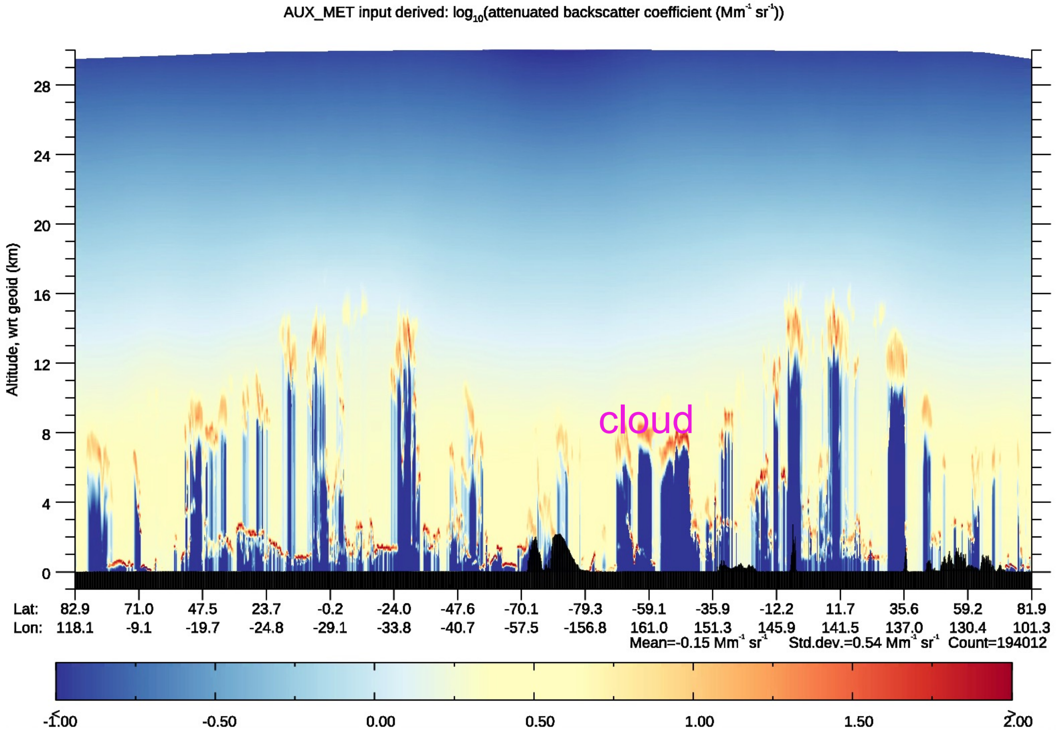

# Level-2B wind processing algorithm overview

- Line-of-sight (**LOS**) or **H**orizontal **LOS** wind components suitable for use in NWP/research
  - Using measurement-level L1B data and calibration products
- Enhancements compared to L1B observations:
  - **Grouping of measurements**: control of horizontal resolution and noise
  - **Classification of measurements**: into different **types** using optical properties (clear/cloudy); to avoid significant Mie contamination of Rayleigh
  - **Accumulation**: of L1B signal of **grouped** and **classified** measurements
  - **Wind retrieval** for different observation types:
    - **Rayleigh-clear; Mie-cloudy**; **Rayleigh-cloudy; Mie-clear**
  - **Rayleigh corrections**:
    - **Temperature**, **pressure** sensitivity (**R**ayleigh-**B**rillouin **C**orrection) using *a priori (AUX_MET)* information
      - without this correction several m/s HLOS wind biases could occur
    - Account for Mie signal on Rayleigh channel using L1B scattering ratio

ECMWF

## … continued

- Uncertainty estimates (dynamic instrument error estimate) and quality flags for each wind result
- Wind observations are essentially independent – however profile also provided pointing to observation index
- Most processing options controllable via settings file (flexible)
- Software freely available and highly portable: https://confluence.ecmwf.int/display/AEOL
- Additional tools in software package:
  - L2B EE to BUFR converter for NWP users
  - Various tools to write products to ASCII
- Aeolus L2B data can be browsed in the ADDF archive (https://aeolus-ds.eo.esa.int) and browsed and plotted by the VirES tool (https://aeolus.services/)

# A very windy day in north-west Europe (10 March 2019)

Photo from near Reading:
apart from low level clouds, sky was clear

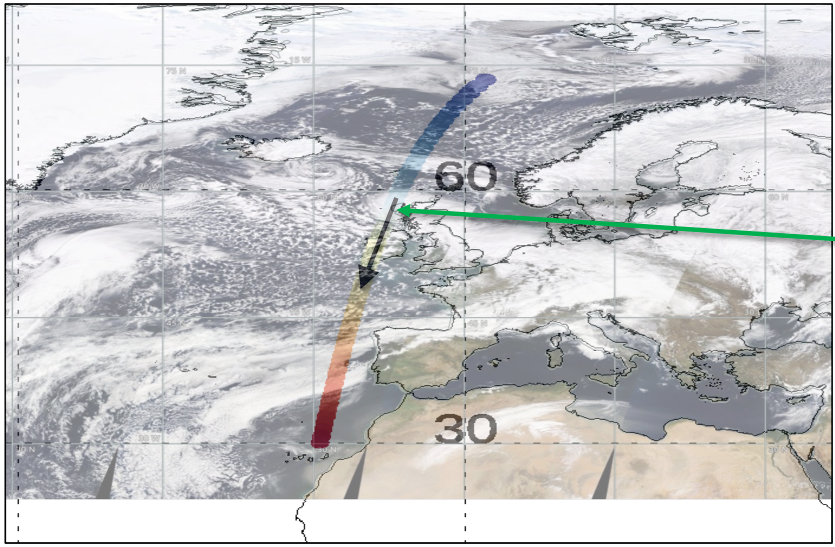


What Aeolus observed (Rayleigh + Mie winds) near the low

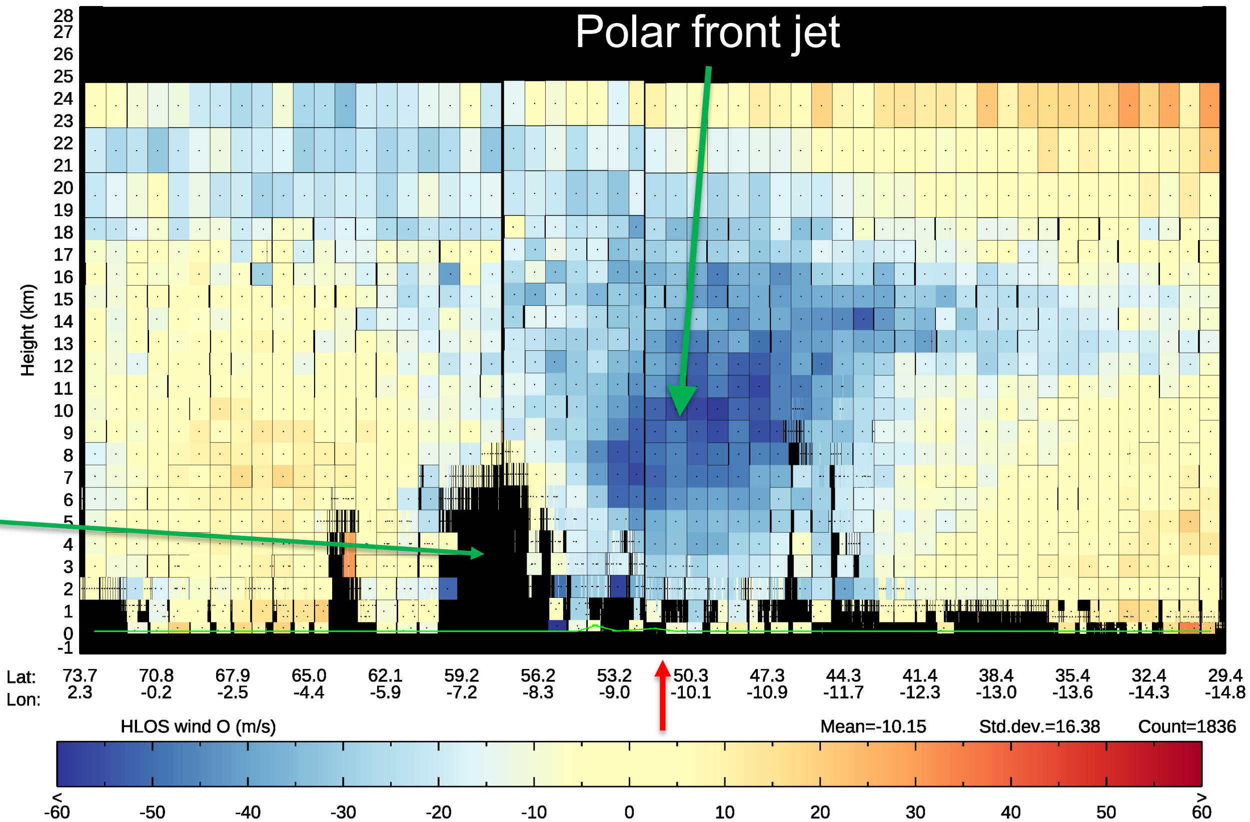

## **A breakthrough in 2019**: explanation for dominant source of Rayleigh wind bias which varies on less than one orbit time-scales was found

- Investigations showed Rayleigh **wind bias**, which varies along the orbit, is strongly correlated with telescope **primary mirror temperatures variations**
- Temperatures vary due to varying Earthshine and the mirror's thermal control
  - Temperature variations correlate with outgoing SW and LW radiation
- *Probable mechanism:* thermal variations alter primary mirror shape, causing angular changes of light onto spectrometer, causing apparent frequency changes
- **Bias correction** using measured telescope primary mirror temperatures was demonstrated to work in offline testing and is being implemented in next processor versions:
  - See references for more details:
  - https://rmets.onlinelibrary.wiley.com/doi/full/10.1002/qj.4142
  - https://amt.copernicus.org/articles/14/7167/2021/amt-14-7167-2021-discussion.html

## Aeolus L2B wind usage in global NWP

- Positive NWP impact was demonstrated
  - Operationally assimilated at ECMWF **from 9 January 2020 to 30 April 2023**
- Other NWP centres found positive impact; operationally assimilated at: DWD, Météo-France, Met Office and NCMRWF
- Being a demonstration mission, still finding ways to improve ground processing algorithms (L1B, L2B, calibration processors) and its usage:
  - **Data quality was not as good as hoped for** i.e. significantly noisier winds, larger biases than expected
  - Lower signal levels -> larger noise
  - Unexpected sources of **wind bias** e.g. primary mirror temperature-gradient sensitivity (0.3K range of gradient across mirror

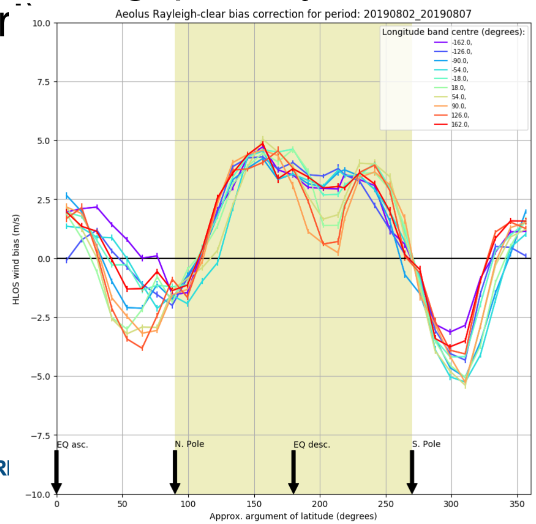


M1 mirror
Ø 1.5 m

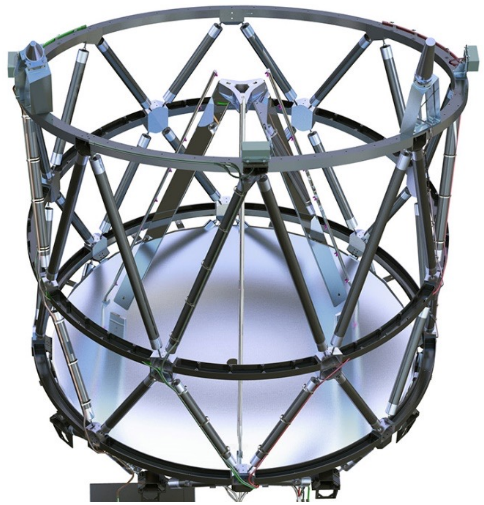

# Rayleigh has large biases which vary with geolocation

Ascending orbit phase **e.g. 6/8/2019 to 7/9/2019**

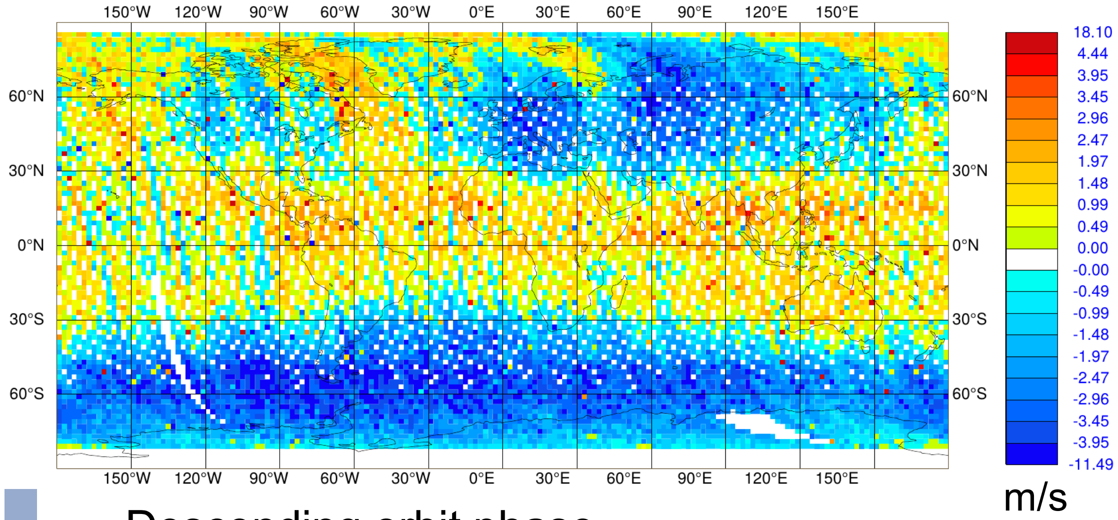


**Average** M1 telescope mirror temperature
Plot from F. Weiler (DLR)

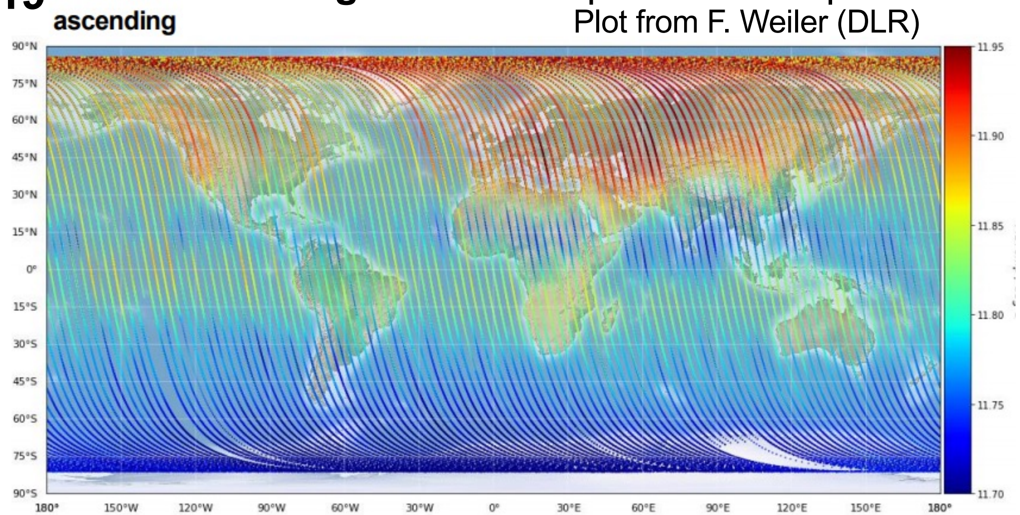


Descending orbit phase

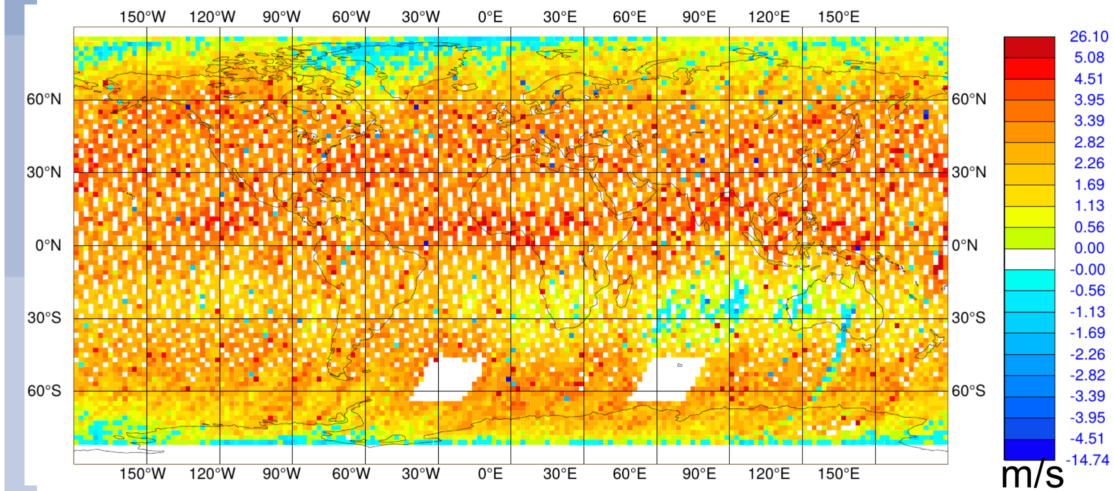


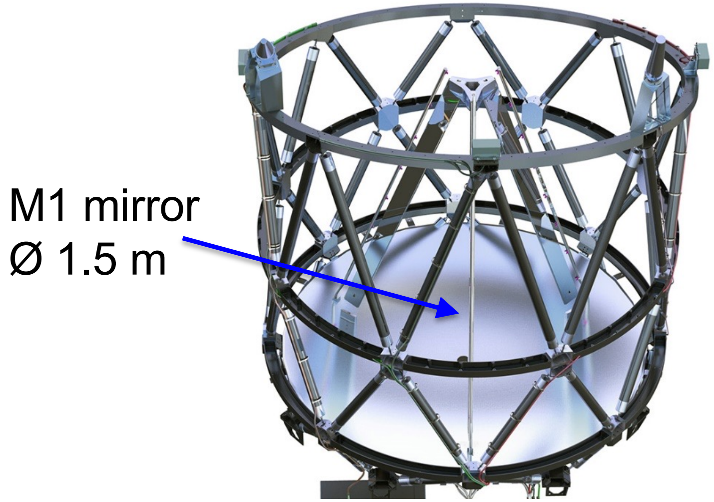

**Regression of <O-B> versus M1 temperature function**

**Best results on 8/8/19 obtained with:**

Outer temp. average: AHT-27, TC-20, TC-21

Inner temp. average: AHT-24, AHT-25, AHT-26, TC-18, TC-19

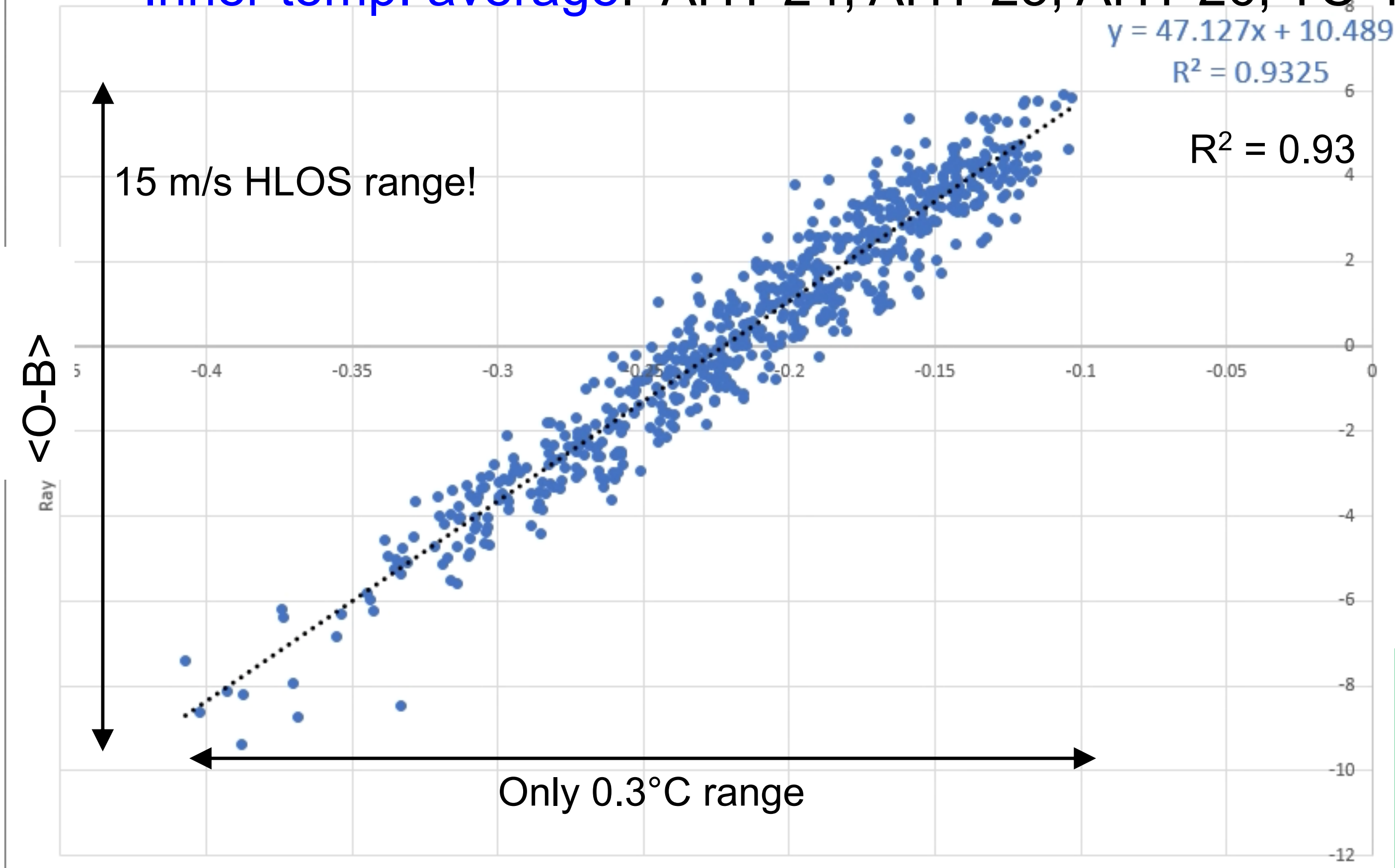


*Outer minus inner M1 temperature function (°C)*

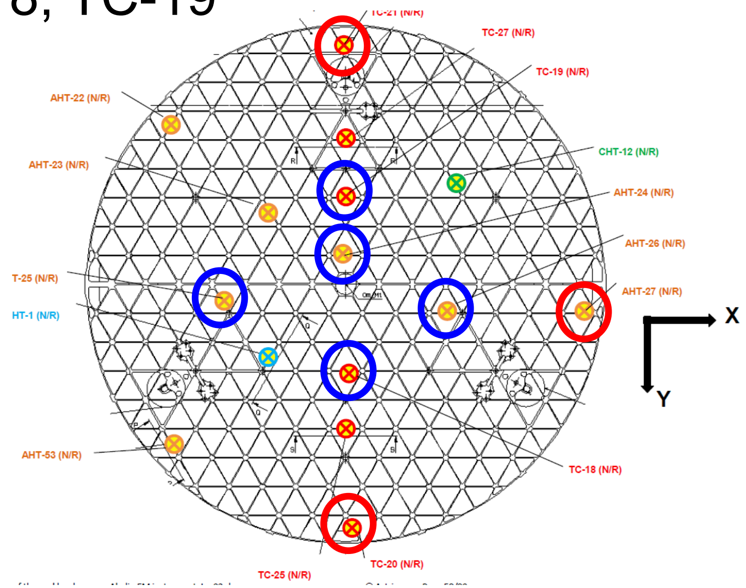


Demonstrates the power of NWP models for helping to determine the source of errors in observations

# Example of bias correction

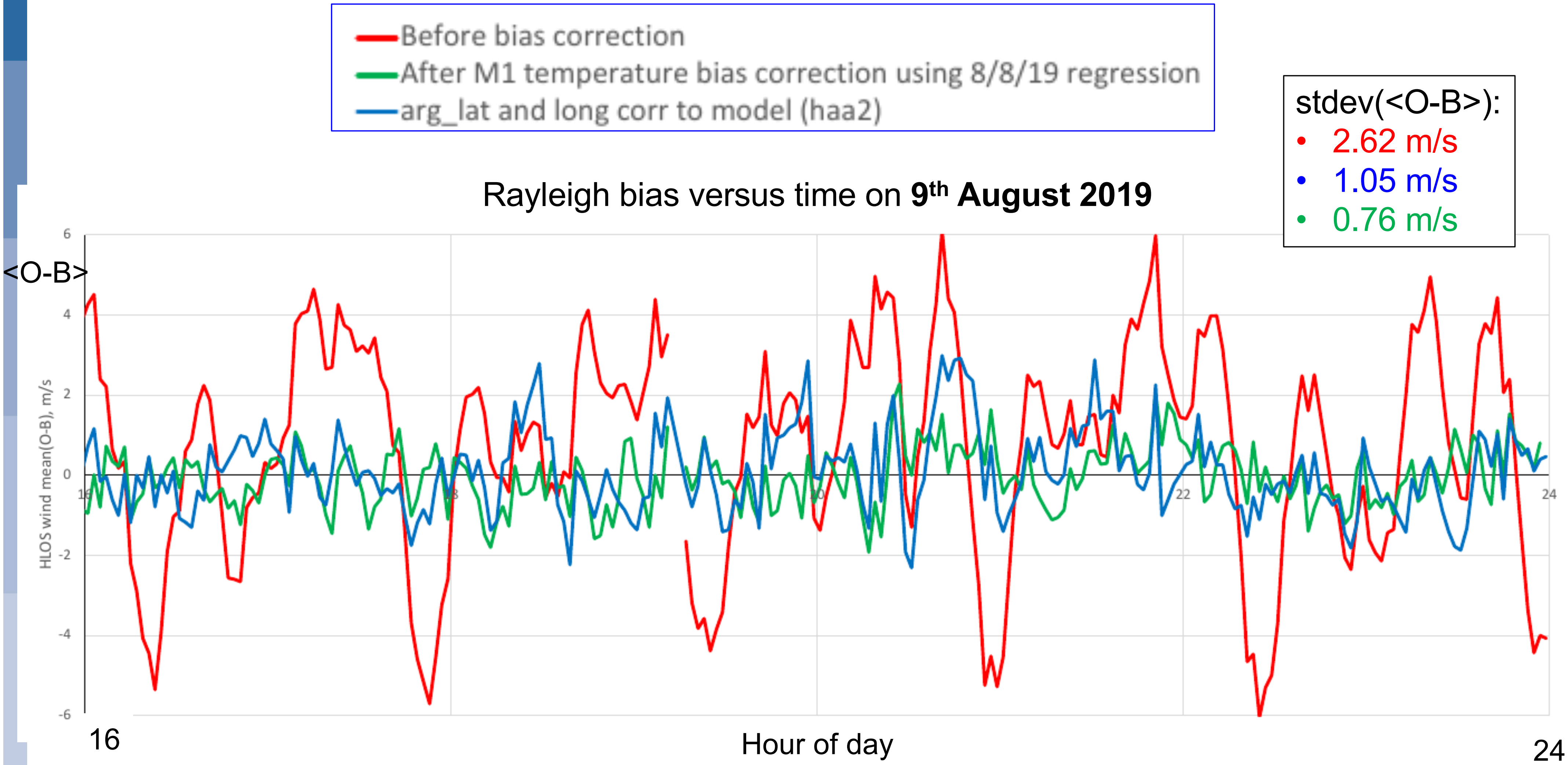

# Bias correction to the ECMWF model

- Implemented bias correction scheme: *<O-B>* vs. *"orbit's argument of latitude" and longitude*
- Updates to bias correction look-up table done typically done every few days in experiments
- Mie biases very stable and do not require the longitude dimension

Example of how **Rayleigh** biases varied during the FM-B period

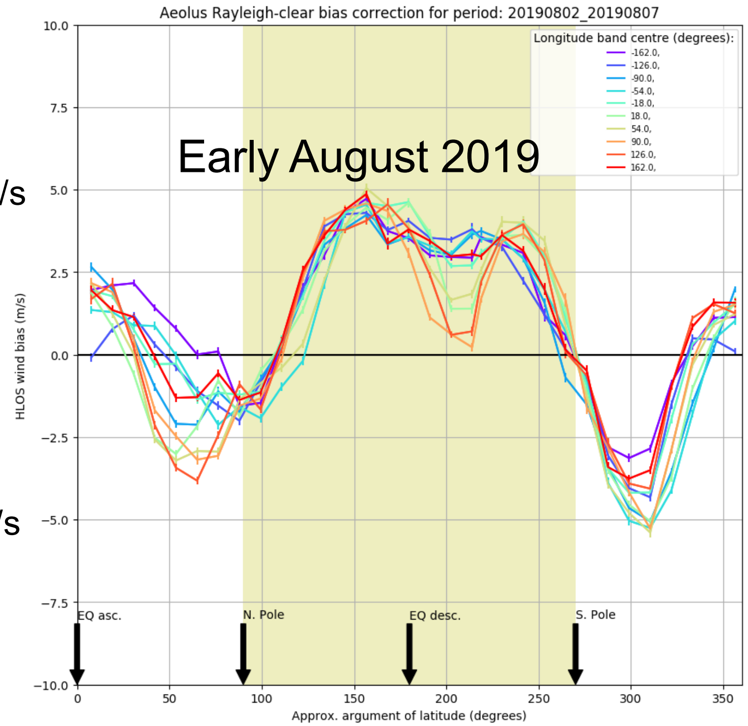


M1 temperature induced biases were larger in boreal summer

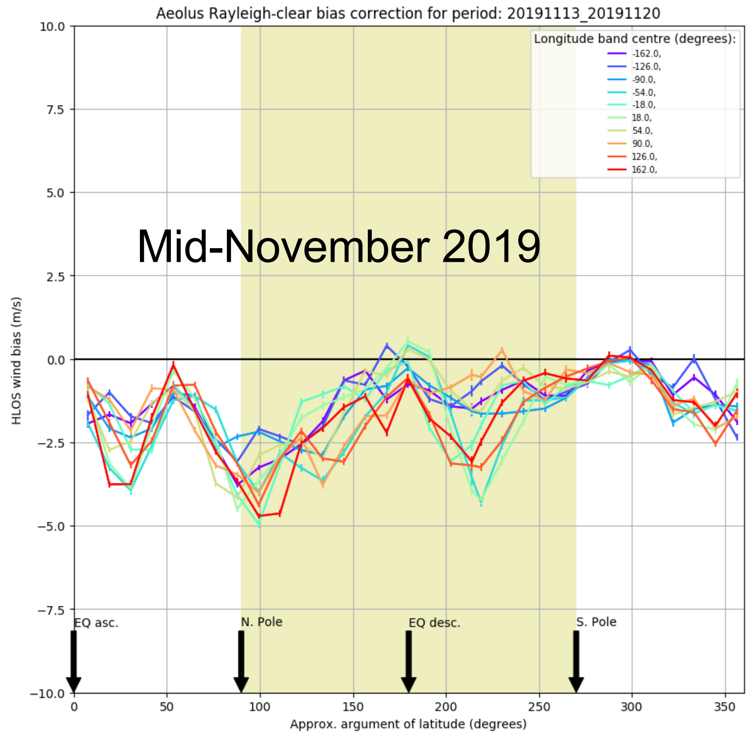

# ECMWF operational relative FSOI (1 Jan to 30 April 2023)

## Data counts by group

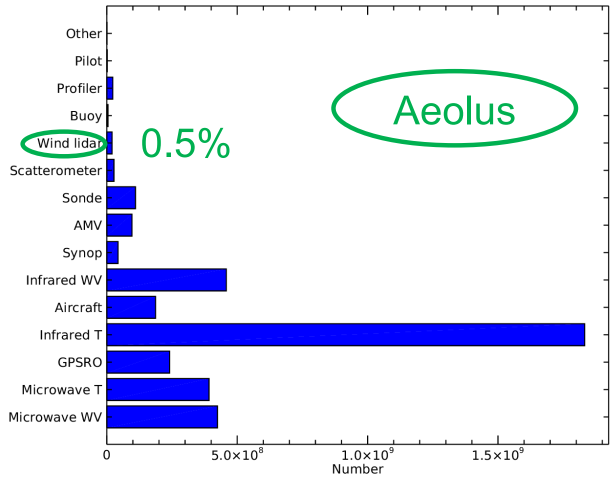


## Relative FSOI (%) by group

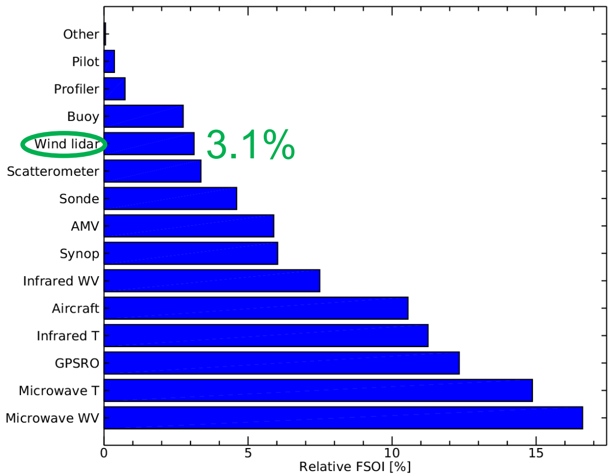


Operational *relative FSOI (%)* *per instrument*

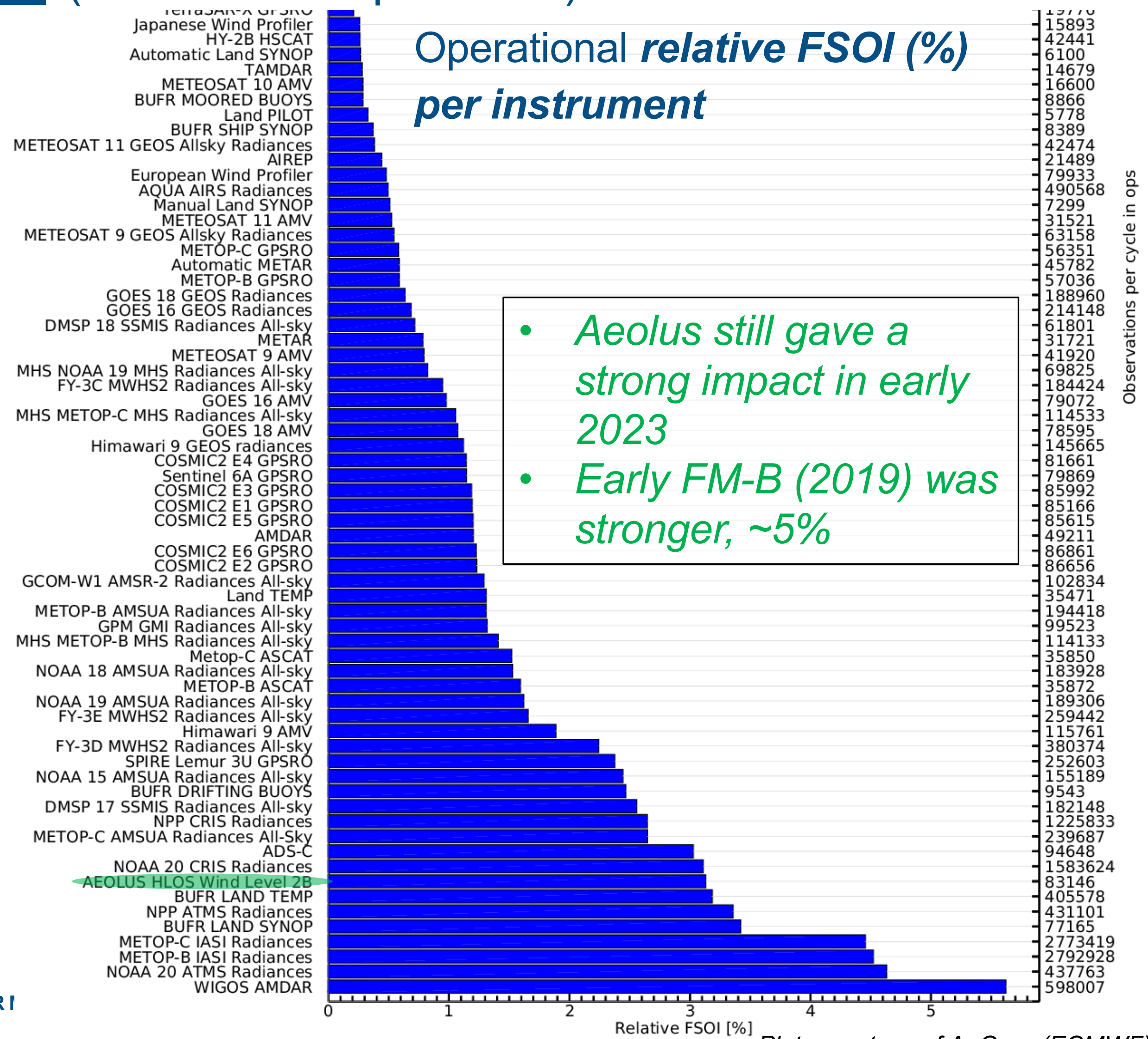


- *Aeolus still gave a strong impact in early 2023*
- *Early FM-B (2019) was stronger, ~5%*

*Plots courtesy of A. Geer (ECMWF)*

# Aeolus does well for one instrument compared to existing multi-instrument satellite systems

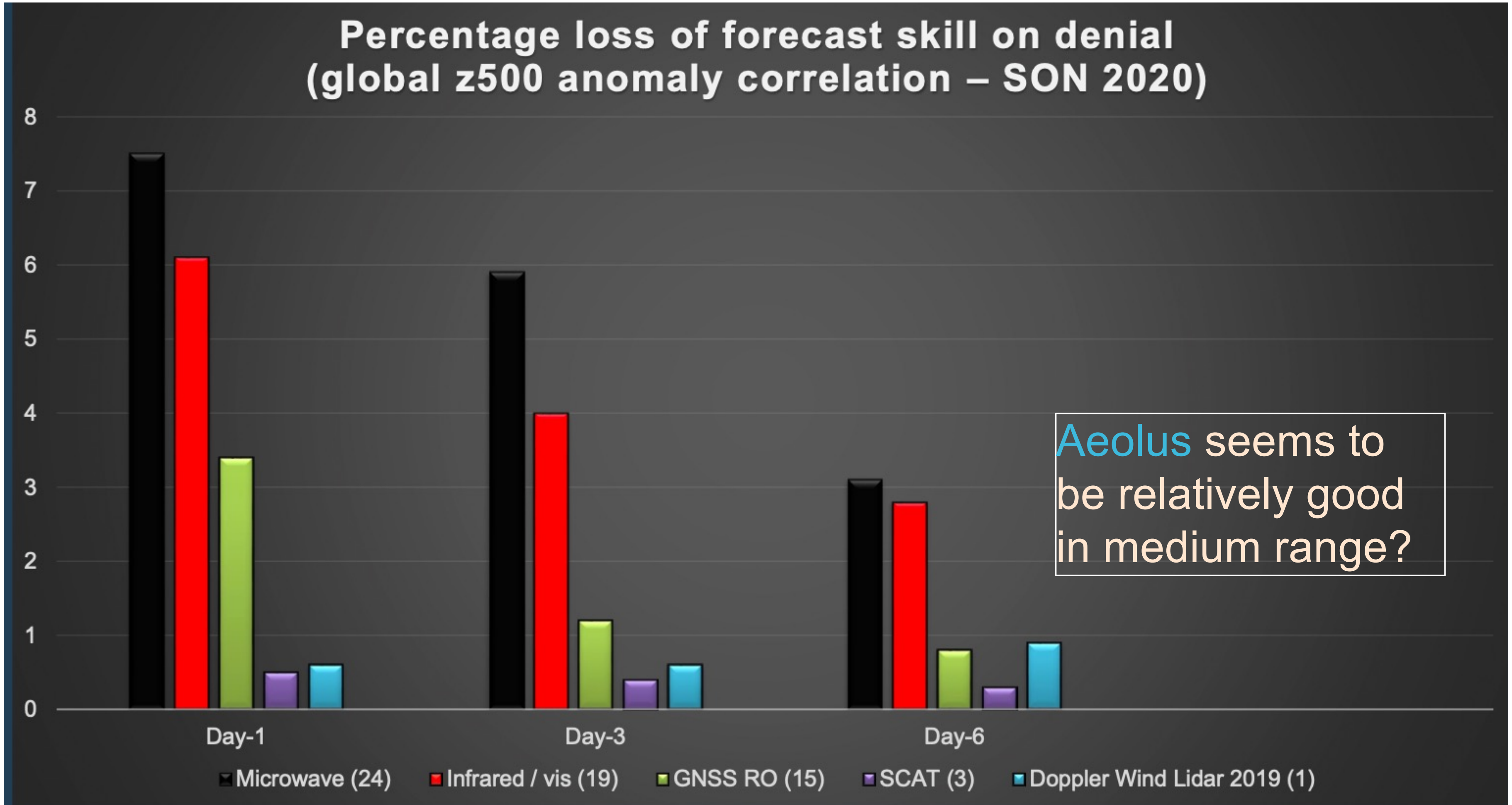


ECMWF

*As shown by Tony on first day!*

## Summary of Aeolus NWP impact at ECMWF

- Aeolus provides a **strong impact** for one satellite instrument
  - Positive impact in most areas and ranges for wind, temperature and humidity
  - Largest impact in tropical and polar UTLS; into medium range

- Shows **importance of *additional* wind** observations in NWP – wind is still not a well-observed variable

# Relative FSOI with **2nd reprocessed dataset**; 3-29 July 2019 (*when Aeolus had its smallest random errors*)

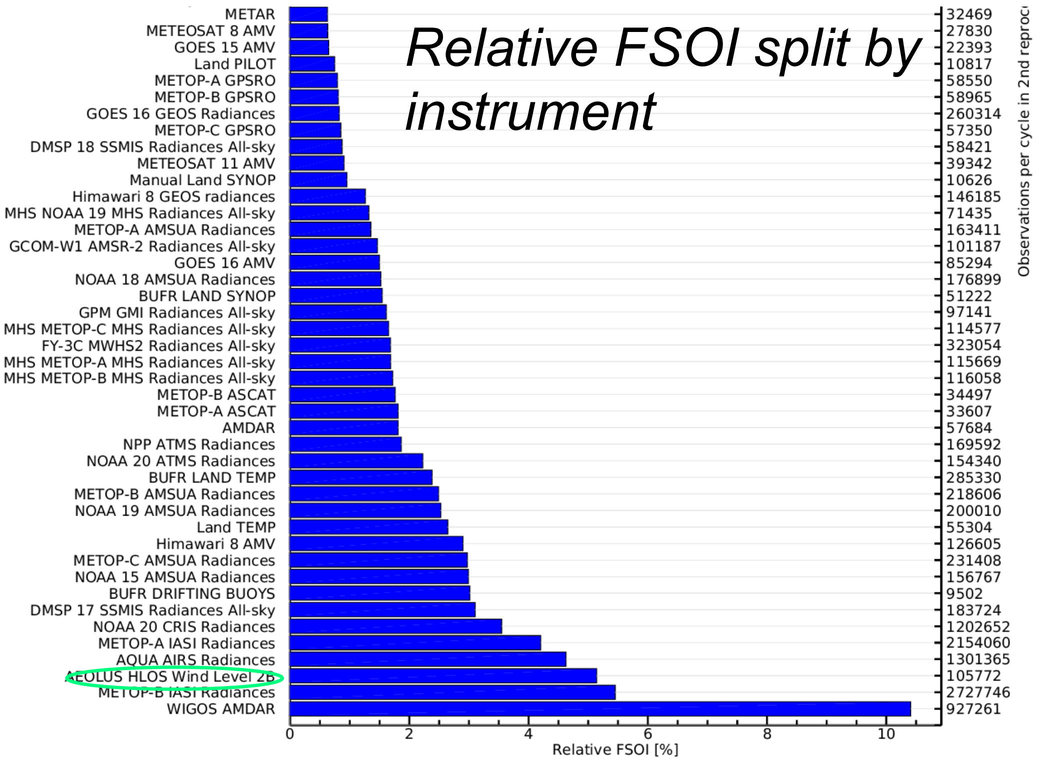


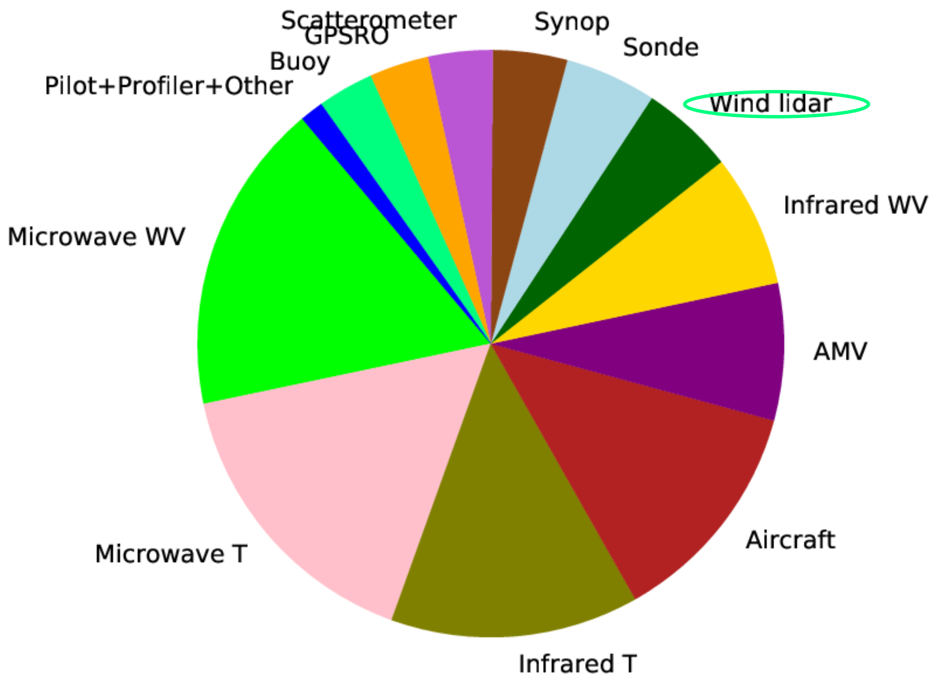


- Aeolus has good impact for **one satellite instrument**
  - When have reasonable Rayleigh-clear random errors

- Wind lidar = Aeolus = 5.1%
- Larger impact than radiosondes for this period